Dipl.-Ing. Martin Lasser, BSc.

Evaluation of GPM-DPR precipitation estimates with WegenerNet gauge data

MASTER'S THESIS

to achieve the university degree of

Diplom-Ingenieur

Master's degree programme: Space Sciences and Earth from Space

submitted to

Graz University of Technology

Supervisor

Assoz. Prof. Mag. Dr.rer.nat Ulrich Foelsche

Institute of Physics, Department Geophysik, Astrophysik und Meteorologie (IGAM)
University of Graz

Graz, October 2018

AFFIDAVIT

I declare that I have authored this thesis independently, that I have not used other than the declared sources/resources, and that I have explicitly indicated all material which has been quoted either literally or by content from the sources used. The text document uploaded to TUGRAZonline is identical to the present master‘s thesis.

Date

Signature

Kurzfassung

Die vorliegende Masterarbeit beruht auf dem Paper "Evaluation of GPM-DPR precipitation estimates with WegenerNet gauge data", das im Oktober 2018 beim Journal Atmospheric Measurement Techniques (AMT) eingereicht wurde. Das Paper bildet den Kern der Arbeit, die folgenden Kapitel dienen als Einleitung in die Thematik, wobei insbesondere auf die GPM (Global Precipitation Measurement) Mission und die verwendeten Messmethoden eingegangen wird.

Der Core Satellite der GPM Mission bietet mittels Beobachtungen eines Zwei-Frequenz Niederschlagsradars (Dual frequency Precipitation Radar - DPR) globale Niederschlagsmessungen. Da die Beobachtungen eines Radars nur indirekt mit der Niederschlagsmenge zusammenhängen, müssen die gesuchten Größen über veschiedene Algorithmen ermittelt werden. Diese Schätzungen benötigen unabhängige Validierungen über eine wahre Referenz am Boden. Das DPR-Instrument liefert drei verschiedene Produkte, eines auf jeder Frequenz (Ku-band, Ka-Band) und ein kombiniertes. Diese Arbeit befasst sich mit der Evaluierung dieser drei Produkte basierend auf Pegelmessungen des Wegener Netzes (WegenerNet), einem lokalen, terrestrischen Netz von 153 Wetterstationen in Südostösterreich. Die Validierung beruht auf einem graphischen und statistischen Teil und verwendet lediglich Daten, an denen Ku-Band und Ka-Band Schätzungen verfügbar sind. Der meteorologische Winter wurde aus technischen Gründen ausgeschlossen. Der Kernpunkt ist die Messung der Variabilität des Niederschlags innerhalb der Fläche des Wegener Netzes mittels des DPR und die Über- bzw. Unterschätzung der Niederschlagsmenge. Die Daten umfassen eine Zeitspanne von vier Jahren, in welchen der Satellit 22 Ereignisse mit Niederschlag detektiert hat. Diese bilden die Grundlage für die Evaluierung. Das Wegener Netz eignet sich als robuste Referenz für solche Evaluierungen, da es eine große Anzahl an Pegelmessungen je Satellitenfootprint liefert, die Auflösung einer einzelnen Pegelmessung etwa doppelt so hoch ist wie die der DPR-Messung und auch der Bias im Netz berücksichtigt ist. In dieser Arbeit sind auch Betrachtungen über die Grenzen von Vergleichen zwischen kleinen, dichten terrestrischen Netzen und Satellitenbeobachtungen enthalten.

Die Ergebnisse zeigen, dass die Radarschätzungen prinzipiell mit dem Wegener Netz zusammenpassen, aber einen Offset aufweisen. Die drei Produkte liefern ähnliche Ergebnisse, wobei Ku-Band Schätzungen und Zwei-Frequenz Schätzungen sehr nahe beieinander liegen. Generell schneiden Ka-Band Niederschlagsmengen am besten ab, das kann allerdings mit der Anzahl an Leicht-Regen Ereignissen erklärt werden.

Abstract

This thesis is based on a paper, titled with same heading, which was submitted to Atmospheric Measurement Techniques (AMT) Journal in October 2018. The paper serves as the core part of the thesis, supplementary information is provided in the introductory chapters, in particular the Global Precipitation Measurement (GPM) mission is described, together with the instruments in space and the data they deliver.

The core satellite of the GPM mission provides precipitation observations measured with the Dual frequency Precipitation Radar (DPR). The precipitation can only be estimated from the radar data, and therefore, independent validations using direct precipitation observation on the ground as a true reference need to be performed. Moreover, the quality and the accuracy of the measurements depend on various influencing factors. In this way, a validation may help to minimise those uncertainties. The DPR provides three different radar rain rate estimates for the GPM core satellite: Ku-band-only rain rates, Ka-band-only rain rates and a product combining the two frequencies. This study presents an evaluation of the three GPM-DPR surface precipitation estimates based on the gridded precipitation data of the WegenerNet, a local scale terrestrial network of 153 meteorological stations in southeast Austria.

The validation is based on a graphical and a statistical approach using only data where both Ku- and Ka-band measurements are available. The data delivered from the WegenerNet are gauge-based gridded rainfall observations; the meteorological winter is excluded due to technical reasons. The focus lies on the resemblance of the variability within the whole network and the over- and underestimation of the precipitation through the GPM-DPR. During the last four years 22 rainfall events were observed by the GPM-DPR over the WegenerNet and the analysis rests upon these rainfall events. The WegenerNet provides a large number of gauges within each GPM-DPR footprint. Its biases are well studied and corrected, thus, it can be taken as a robust ground reference. This work also includes considerations on the limits of such comparisons between small terrestrial networks with a high density of stations and precipitation observations from a satellite.

Our results show that the GPM-DPR estimates basically match with the WegenerNet measurements, but absolute quantities are biased. The three types of radar estimates deliver similar results, where Ku-band and dual frequency estimates are very close to each other. On a general level, Ka-band precipitation estimates deliver the best results due to the high number of light rainfall events.

Contents

Part I

Introduction

Precipitation is one of the most fundamental items of understanding the system Earth. It is not only used in weather forecasting but also in a variety of scientific fields that touch the global water cycle, such as hydrology, studies on climate change, weather phenomena etc. Understanding the global precipitation cannot be achieved by terrestrial means, and therefore, satellite missions, such as the Global Precipitation Measurement (GPM) mission aim to give consistent and comprehensive information about Earth's global rainfall. Precipitation can be measured by different techniques, widespread ones are the usage of a weather radar for an indirect measurement or direct observations by employing gauges. In this work radar estimates from the GPM mission are evaluated using gauge observations in the WegenerNet.

The GPM mission targets to provide consistent and comprehensive information about Earth's global precipitation with a high temporal and spatial resolution. Global rainfall maps are determined every three hours to evaluate the precipitation flow. The results are utilised in weather forecasts, flood predictions and river managements, studies on global change and climate variations as well as the assessment of the global water cycle (see JAXA, 2017). The mission is led by the National Aeronautics and Space Administration (NASA) and the Japan Aerospace and Exploration Agency (JAXA). The GPM Core Observatory (GPM-CO) satellite, which is the main development for the mission, is equipped with an active Dual frequency Precipitation Radar (DPR) and a passive GPM Microwave Imager (GMI). Together with a constellation of partner satellites from international space and weather agencies, such as the National Oceanic and Atmospheric Administration (NOAA), the Centre national d'études spatiales (CNES) and the Indian Space Research Organisation (ISRO) or the European Organisation for the Exploitation of Meteorological Satellites (EUMETSAT), it provides global-scale precipitation data. Next to its own measurements, it serves as a reference for unifying the data from the partner satellites (Skofronick- Jackson et al., 2016). The main instrument is in principle a weather surveillance radar operating on two frequencies to map weather events across its swath. The two frequencies allow to estimate the sizes of precipitation particles and detect a wider range of precipitation rates than a single frequency. The microwave imagers augment the core satellite and enable a high temporal resolution for global precipitation maps. In this study, solely the surface rain rate estimates derived from DPR on board the GPM-CO are evaluated and compared to the rain-gauge-based gridded data from the WegenerNet. The WegenerNet is a local scale dense terrestrial network of meteorological stations in the Feldbach region of southeast Austria. It consists of 153 meteorological stations, constructed in an area of roughly 20˜km˜×˜15˜km, forming a structured grid with a cell area for each station of about 2 km^2. Each station measures meteorological quantities such as temperature, humidity and precipitation. In all stations a tipping bucket rain gauge instrument with a volume of 0.1 mm is used, however, only twelve contain a heating device, and are therefore able to reliably measure winter precipitation. Since satellite estimates provide only measurements at points in time and not accumulations, one prerequisite for evaluating with terrestrial gauge data is that the accumulations are as short as possible, but still providing high quality information. Even though theWegenerNet is of very small scale, it provides in its 5 minutes accumulations considerably more and better information than the GPM-DPR, especially because of the high spatial resolution in the covered area. Therefore, it is possible to evaluate every DPR footprint based on the information of 8-10 or even more stations. The drawback is the small number of fly-overs with actual precipitation, which allow only an event-based analysis. This analysis is done using graphical support and quantifying the quality of the DPR estimates using statistical tools that are usually employed in weather forecast validation. The analysis itself

is explained in the paper.
The thesis is structured in the following sections:

- Part II gives an overview about the GPM mission, its goals and data. The following
- Part III is dedicated to the GPM-CO satellite and its instruments. In
- Part IV the WegenerNet is outlined, providing additional information to the summary in the paper, which is incorparated in
- Part V: **Evaluation of GPM-DPR precipitation estimates with WegenerNet gauge data** (Lasser, M., O, S., and Foelsche, U.) The paper is composed of five sections:
  - 1. Introduction
  - 2. Data (2.1 WegenerNet, 2.2. GPM-DPR, 2.3. Selected Data)
  - 3. Methodology
  - 4. Results (4.1. Evaluation of all rainfall events, 4.2. Analysis of example rainfall events)
  - 5. Conclusions

An outlook with some notions on future improvements is part of the paper's last section with concluding remarks. Precipitation maps for all events that were evaluated are attached after the paper.

Part II

GPM satellite mission

The GPM satellite mission's goal is to provide a high resolution global rain map every three hours in near-realtime exploiting the data from multi-satellites. These data help to improve weather forecasts and flood predictions. Moreover, agricultural production forecasting and water resource management, such as river water or agricultural water, shall be supported. Likewise, the view on longer time spans of the global precipitation shall improve the climate change assessment and monitor variations in rainfall and rain areas due to climate change and global warming.
The mission is led by the National Aeronautics and Space Administration (NASA) and the Japan Aerospace and Exploration Agency (JAXA). It is the successor mission of the Tropical Rainfall Measurement Mission (TRMM) and consists of a Core Observatory, equipped with an active Dual frequency Precipitation Radar and a passive Microwave Imager, and a number of partner satellites with a passive microwave sensors mounted. Together with these satellites the global coverage is achieved with a temporal resolution of less than three hours. The constellation satellites fly mainly in a sun synchronous orbit and between 600 and 800 km of altitude. The following spacecraft are members (or contributing data members) of the GPM constellation (JAXA, 2017).

Table II.1: Constellation satellites of the GPM mission

Satellite	Operator	Sensor	Orbit	Lifetime
GPM-CO	NASA/JAXA	DPR, GMI	400 km, 65°	2014-
TRMM	NASA/JAXA	PR, MTI	380 km, 35°	1997 - 2014
GCOM-W1[1]	JAXA	Radiometer	700 km, 98°	2012-
DMSP F15[2]	NOAA	Microwave Imager	840 km, 98°	1999 -
DMSP F16	NOAA	Microwave Imager Sounder	840 km, 98°	2003 -
DMSP F17	NOAA	Microwave Imager Sounder	840 km, 98°	2006 -
DMSP F18	NOAA	Microwave Imager Sounder	840 km, 98°	2009 -
DMSP F19	NOAA	Microwave Imager Sounder	840 km, 98°	2014 - 2016
Megha Tropiques	CNES/ISRO	Multi-Frequency Microwave Scanning Radiometer	865 km, 20°	2011 -
MetOp-A[3]	EUMETSAT	Microwave Humidity Sounder	817 km, 99°	2006 -
MetOp-B	EUMETSAT	Microwave Humidity Sounder	817 km, 99°	2012 -
MetOp-C	EUMETSAT	Microwave Humidity Sounder	817 km, 99°	2018 -
NOAA-18	NOAA	Advanced Technology Microwave Sounder (ATMS)	854 km, 99°	
NOAA-19	NOAA	ATMS	860 km, 98°	
NOAA-20 (JPSS-1[4])	NOAA	ATMS	830 km, 98°	
JPSS-2	NOAA	ATMS	-, -	2022 -
Suomi-NPP[5]	NASA/NOAA	ATMS	824 km, 99°	2011 -

One of the main tasks of GPM-CO is to provide a reference to unify the data from the whole constellation for consistent precipitation rates from all satellites and sensors.

[1] Global Change Observation Mission Water
[2] Defense Meteorological Satellite Program
[3] Meteorological Operational Satellite
[4] Joint Polar Satellite System
[5] National Polar-orbiting Partnership

1 Data

Satellite mission data are divided into different levels, starting from most basic data (Level 1A data), such as telemetry data and raw observations, which are usually not published. Level 1 data continue with calibrated, time tagged, geolocated observations. These may be published (Level 1B or Level 1C) as it is the case for most of the GPM data; some constellation satellite data is not provided for public usage (in particular parts of the DMSP data) . Level 2 data, which are employed in this work, contain the geophysical parameters derived from the observations. In this case precipitation rates retrieved from the dBZ values the DPR observes. Level 3 data comprise the geophysical quantities from Level 1 or Level 2 data in a spatially and/or temporally re-sampled manner. Table II.2 shows the GPM data levels and the corresponding products.

Table II.2: Overview of the GPM data levels and products

Level 1	A	unprocessed instrument data at full resolution
	B	time referenced, and annotated with auxiliary information
	C	including radiometric and geometric calibration and georeferencing
Level 2	2A-Ku	DPR Ku-only single orbit rainfall estimates
	2A-Ka	DPR Ka-only single orbit rainfall estimates
	2A-DPR	DPR Ku and Ka single orbit rainfall estimates
	2A-GPROF-const.	Single-orbit rainfall estimates from each passive-microwave instrument in the GPM const.
	2A-GPROF-GMI	GMI single-orbit rainfall estimates
	2B-CMB	Combined GMI + DPR single orbit rainfall estimates
Level 3	IMERG	Rainfall estimates combining data from all passive-microwave instruments in the GPM const.
	3-CMB	Combined GMI + DPR Rainfall Averages
	3-DPR	DPR rainfall averages
	3-GPRO	GMI rainfall averages
	3-GPROF	Gridded rainfall estimates from each microwave imager in the GPM const.

The master list of all GPM and GPM constellation products can be found at:
`https://pps.gsfc.nasa.gov/Documents/Master_List_of_PPS_Data_Products.html`.
The data are delivered via NASA's PMM server (`http://pmm.nasa.gov/data-access/`). It comes in the Hierarchical Data Format (HDF5), which is the prescribed format for NASA's EOS (Earth Observing System) programme. The data are given scene-wise, where one scene corresponds to one orbital revolution.

Part III

GPM-CO

The GPM-CO is the primary satellite of the GPM mission, it is a joint partner project of NASA and JAXA. It targets to provide global precipitation estimations like its predecessor, the TRMM satellite, which was launched in 1997 and operated until 2015. The GPM-CO was launched in 2014 with a H-IIA Rocket Vehicle at Tanegashima Space Center. Due to the overlap in time with TRMM the in-space data validation with both satellites was achieved. GPM-CO employs for its observations a Dual frequency Precipitation Radar - in contrast to the TRMM, which utilised only a single frequency band (Ku-band) - and a Microwave Imager. The instruments are described in the following sections. The design life of GPM-CO is three years and two months for the satellite, the DPR and the GMI; this was surpassed in April 2017. Fuel lasts for at least five years, depending on the solar activity and the number of orbital maneuvers that need to be performed. GPM-CO flies in a circular orbit of 400 km altitude, with a non sun-synchronous pattern, and 65° of inclination, opposed to its predecessor TRMM, which had an inclination of 35°, only observing the tropical rainfall. Thus, the GPS-CO covers almost the whole inhabited Earth, and includes various kinds of precipitation to be detected, from heavy in the tropics to very light in the mid-latitudes. Furthermore, the orbit overlaps with the constellation satellites and is chosen to feature minimal ground track repeat. Consequently, a frozen-orbit design is applied in case of GPM, where the altitude variations due to the gravity field are as little as possible. The requirement is, that the orbit must not deviate from the reference orbit by more than one kilometre for the whole mission lifetime, while reducing orbital maneuevers to a minimum.
The two major contractors NASA and JAXA share their responsibilities for the GPM-CO according to Table III.1.

Table III.1: Responsibilities between NASA and JAXA for the GPM-CO

	NASA	JAXA
Launch		✓
Satellite bus	✓	
Tracking and control (mission operation)	✓	
DPR		✓
GMI	✓	
Data processing	✓	✓
Data distribution	✓	✓

The data distribuition task is executed by both parties to gain as much outreach as possible. Both deliver the same products. A summary of the most important facts on the satellite is given in Table III.2. The costs only include NASA's contribution, JAXA's monetary effort was not published. The size of the satellite is the extent in space with the solar panels folded out. The satellite istself is displayed in Fig. III.1. Note the size of the radar antennas and the high gain antenna, which is not Earth-pointing, because of the utilisation of the Tracking and Data Relay Satellites (TDRS) system.

Table III.2: Fact sheet of the GPM-CO

name	GPM-CO
operator	NASA/JAXA
mass	3850 kg
size	13 m × 6.5 m × 5 m
orbit	non-sun-synchronous, circular
altitude	407 km
semi major axis	6776 km
inclination	65°
eccentricity	0.00010
orbital period	93 min
mission start	Febuary, 27th, 2014
	operational since then
costs (GPM mission)	978 Million $ (NASA)

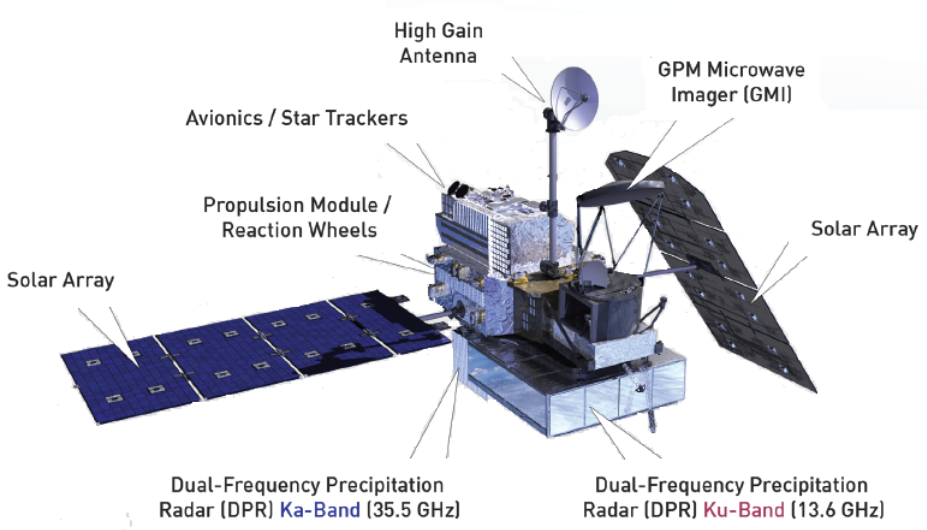

Figure III.1: GPM-CO satellite and its main instruments[6]

The flight direction is pointing along the GMI, i.e. the almost upright solar array is one the lefthand side of the satellite in flight direction.

1 Instruments

Dual Frequency Precipitation Radar (DPR)

The DPR builds together with the GMI the main payload of the GPM-CO. It consists of two nadir-pointing radars with different frequency bands, Ku-band at 13.6 GHz and Ka-band at 35.5 GHz, to measure the the structure of precipitation in three dimensional layers on a global scale, which means it must be capable to detect heavy tropical rainfall and light precipitation in the mid-latitudes. Furthermore, the DPR observations are used as a reference for unifying the different observation from the constellation satellites. The Ku-band Precipitation Radar (KuPR) aims to detect heavier rainfall, whereas the Ka-band Precipitation Radar (KaPR) is sensitive to light precipitation. Simultaneous observation between KuPR and KaPR allow a

[6]Source: JAXA/NASA (2014)

combination of the two radar instruments. The design life of the DPR is three years and two months (see JAXA, 2017). The DPR employs a Variable Pulse Repetition Frequency (VPRF) technique to obtain the same accurays over its whole orbit, since the 65° inclination leads to altitude variations of about 20 km. Figure III.2 shows the observation geometry of the GPM-CO.

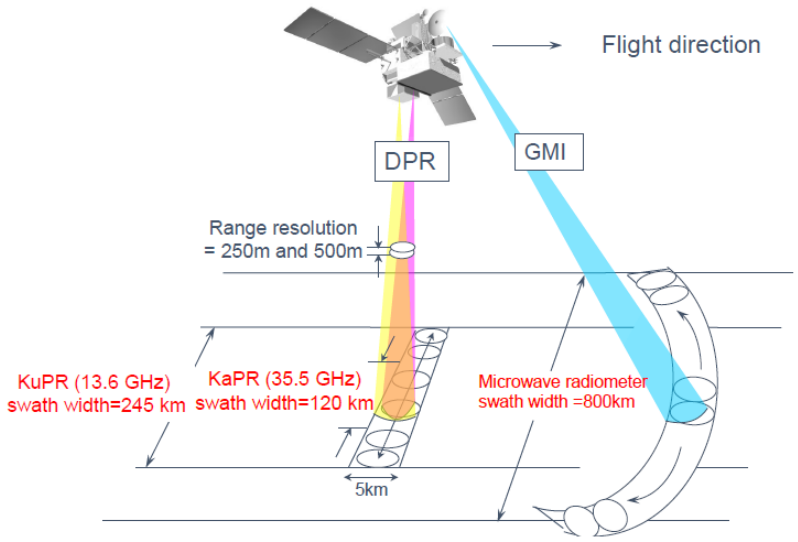

Figure III.2: GPM-DPR observation principle with the DPR and the GMI[7]

The KuPR has 49 beams and covers an area of 245 km across its swath (Normal Scan pattern, i.e. Ku-NS), the KaPR covers 125 km with 25 beams in the Matched Scan pattern (Ka-MS). These beams coincide with the 25 inner beams of the Ku-NS with am accuracy of less than 1 km. Furthermore, KaPR incorporates a High Sensitivity Scan pattern (Ka-HS) with 24 beams and 120 km swath width, where the beams are interlaced between the MS pattern. Figure III.3 displays the different scan patterns.

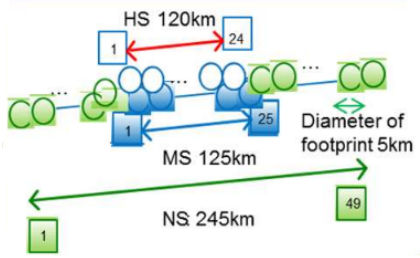

Figure III.3: GPM-DPR observation principle with the DPR and the GMI[8]

The footprint one radar beam projects on the Earth's surface has a diameter of 5.2 km (horizontal resolution) for Ku- and KaPR. The vertical resolution is 250 m for NS and MS, which means that every 250 m a precipitation layer can be esimated, the maximum observable altitude is 18 km. A brief overview of the main characteristics of the DPR is given in Table III.3, which summarises Iguchi (2017).

[7]Source: Iguchi (2017)
[8]Source: JAXA (2017)

Table III.3: DPR-instrument characteristics

	KuPR	KaPR
Frequency	13.597 & 13.603 GHz	35.547 & 35.553 GHz
Beams (scan pattern)	49 (NS)	25 (MS), 24 (HS)
Swath width	245 km	125 km (MS), 120 km (HS)
Horizontal resolution	5.2 km at nadir	5.2 km at nadir
Vertical resolution	250 m	250 m or 500 m
Observable range (altitude)	18 km to -5 km	18 km to -3 km
Min. resolution	18 dBZ (~ 0.5 mm/h)	12 dBZ (~ 0.2 mm/h)
Accuarcy	1 dBZ	1 dBZ
Mass	365 kg	300 kg
Size	2.4 m × 2.4 m × 0.6 m	1.44 m × 1.07 m × 0.7 m
Power consumption	383 W	297 W

The remote sensing with RADAR (RAdio Detection And Ranging) is based on the principle that a known pulse of radio waves is emitted (active instrument) and its echoes from objects or targets are then measured. For the initally intended task of detection and ranging, the distance to the target can be derived from the time the pulse travels, the direction to the target is given by the direction of the radio waves. In radar meterology the aspect, that the echo power depends on the size and number of the targets, is added to the considerations.

The radar equation for meterology reads as follows

$$P_r = P_t \frac{G^2 \lambda^2 \sigma}{64 \pi^3 r^4}, \tag{III.1}$$

where P_r is the received power, P_t the peak power transmitted by the radar, G the gain of the antenna, λ the wavelength, r the distance to the target, and σ the radar cross section of the target. The received power is highly dependent on the antenna. A high antenna gain is necessary, which makes the antenna highly dependent on the direction - a challenge for spaceborne radars - and the wavelength (the longer, the better, usually ground radars employ wavelengths in the S- or C-band, cf. Iguchi, 2003). The distance to the target decreases the received power by the magnitude of four, which is one of the most delicate points of spaceborne radar observations.

For a distributed target in the radar beam, such as precipitation, the pulse length and the reflectivity of the target η need to be included in the consideration. The radar reflectivity depends on the emitted wavelength and the sizes (D) and concentration of the condensated water and its respective thermodynamic phase. Under the assumption that $\lambda \gg D$ (Rayleigh scattering), the reflectivity is given by

$$\eta = \frac{\mid K \mid^2 \pi^5}{\lambda^4} Z \tag{III.2}$$

where K is the dielectric factor, around 0.9 for water and 0.2 for ice. Z is the radar reflectivity factor of the precipitation, the most fundamental value for precipitation estimation. It may be written in terms of the Drop-Size Distribution (DSD) as

$$Z = \int_0^\infty N(D) D^6 dD \tag{III.3}$$

where $N(D)$ is the number of drops per unit volume with diameters in the interval dD. Since the Z-value is

dependet on the sixth power of the drop diameter, a logarithmic scale is applied.

$$dBZ = 10\log(\frac{Z}{Z_0}), \tag{III.4}$$

where $Z_0 = \frac{1\text{mm}^6}{\text{m}^3}$. The DSD is the distinctive signature of a cloud and can then be transformed to rainfall. The simplest relationship is

$$R = \int_0^\infty \frac{1}{6} N(D)\pi D^3 v(D) dD, \tag{III.5}$$

where the amount of rainfall R is related to the number of drops N, their volume $\frac{\pi D^3}{6}$ and the falling speed v.
Ususally clouds have a unimodal DSD. Convective and stratiform rainfall can be expressed by the satellites DSD estimation quite accurately, orographic rain shows large discrepancies.

For satellite-based radar several constraints have to be considered: The hardware must fit the satellite, which decreases the antenna size drastically (lower gain) and the power to transmit the radio wave is limited. The realisation of a good horizontal resolution together with a high antenna gain makes it necessary to use short waves (Ku-band or Ka-band), which, however, suffer from attenuation (rain, snow, water vapor, cloud liquid water, and oxygen molecules) thats needs to be corrected. The footprint size is roughly

$$fp_{diameter} = \frac{c_1 \lambda r}{D}, \tag{III.6}$$

where $c_1$is a constant, that depends on the antenna illumination (1.2) , r is the distance to the surface and D is the antenna diameter (cf. Iguchi, 2017). Thus, the smaller the wavelength λ emitted, the better the horizontal resolution. For a five kilometre footprint diameter, 400 km of altitude and a one metre antenna, the wavelength would be around 28 Ghz.
Other limiting factors are the data rate, on board memory, the power consumption and especially the distance to the target of more than 300 km, which decreases the power of the echo drastically. Furthermore, the satellite observes the rain from above, thus observing the upper layers first (first ice, then snow, then a melting layer and lastly the rain). The satellite is a moving platform for the radar, which gives a poor sampling in time on a specific location, in case of the WegenerNet the GPM-CO passes aorund 10 times a month. Various rain systems with different characteristics cannot be captured well (e.g. orographic rain). This needs to be taken into account when performing a validation.

GPM Microwave Imager

The GMI is a passive instrument that employs a multi-channel, conical- scanning, microwave radiometer to measure the total precipitation within all cloud layers, including light rain and snowfall (JAXA, 2017) It observes the intensity of microwave energy that is emitted by rain and snow. The GMI radiometer is a light instrument with 166 kg. It is composed of a scanning antenna with 1.22 m diameter that collects the microwaves from the scene and reflects them to a detector, which procesess the radio waves. It comprises 13 microwave channels with frequencies between 10 GHz an 183 GHz, where the lower frequencies (10 GHz to 89 GHz) measure heavy rainfall and the high- frequency channels (166 GHz to 183 GHz) sense moderate-to-light precipitation. The footprints are of elliptical shape due to the off-nadir view, and their size is frequency dependent and between 18 km^2 and 600 km^2. The scanning antenna rotates with 32 rpm to collect microwave

data along the circular track it traces on the ground over a centred 140 degree sector, which corresponds to a swath of 904 km on the Earth's surface. The GMI is off-nadir pointing with an angle of 48.5 degrees. Calibration is done via observation of cold space as well as observation of a hot calibration target mounted on the satellite. Only the central portions of the GMI swath overlap the DPR swaths (max. 245 km swath width). These overlapping observations have a speration in time of about 67 seconds due to the geometry, since the GMI is highly off-nadir looking in front of the satellite. These measurements within the overlapped swaths are important for improving precipitation retrievals, in particular, the radiometer-based retrievals. The GMI is taken as a reference for unifying the microwave sensing data from the constellation satellites.

Other subsystems

For the sake of completeness the other subsystems of GPM-CO are mentioned here, cf. ESA (2018).

Attitude Determination and Control Subsystem (ADCS) The GPM-CO has an IRU (Inertial Reference Unit) and two wide-angle star trackers mounted as main attitude sensors. In general a star tracker takes a picture from the starry sky and detects stars using image processing. After some corrections, the detected stars are matched to a star catalogue, from which the current attitude of the satellite can be derived. The IRU uses gyroscopes on all three axes to measure changes in the attitude. Two magnetometres units are mounted on GPM-CO to determine the spacecraft's attitude relative to Earth's magnetic field. Attitude control is primarily accomplished by a reaction wheele.
A GPS receiver unit is used to derive the spacecraft's position, velocity and altitude for navigational purposes as well as for antenna pointing and science data processing.

Command and Data Handling Subsystem (C&DHS) The C&DHS performs the task of command reception and execution, spacecraft control, housekeeping and payload operations. Housekeeping data and science data are either processed and downlinked in realtime or stored in a solid-state recorder before downlink.

Electrical Power Subsystem (EPS) The EPS of GPM-CO consists of two solar arrays with four panels on each array. Each panel comprises around 1000 Gallium-Arsenide solar cells. The total solar cell area is 26.5 m^2.

Thermal Control Subsystem (TCS) GPM-CO has an active and passive thermal control. Active thermal control uses heaters, heat rejection systems and temperature sensors to maintain the operating temperature. The heat is transported via heat pipes and rejected via radiators attached on the side of the spacecraft that never faces the sun. Passive thermal control mainly prevents from sunlight heating the satellite.

Reaction Control Subsystem (RCS) The RCS onboard of GPM-CO is made of a chemical propulsion system with high-purity hydrazine fuel (545 kg onboard) and reaction wheels for orbit and attitude control. Twelve thrusters are mounted on the spacecraft, however, only four are used for orbit maneuvers (drag compensation), the others perform the attitude control. The orbit maneuvers are executed roughly every 13 days.

Radio frequency communications subsystem (RF comm) The RF comm of the GPM-CO includes a S-band communication system for information exchange with the ground. It makes use of the TDRS to

obtain high downlink data rates. The downlink data rate is around 230 kbit/s for housekeeping/telemetry data and realtime payload and 2.3 Mbit/s for stored science data. Mission Operation Center (MOC) is the Goddard Space Flight Center (GSFC) of NASA. Up-/downlink station is White Sands/NM.

Part IV

WegenerNet

The WegenerNet is a long-term weather and climate observation network providing its measurements at a very high resolution. It has been deployed in 2006 by the Wegener Center for Climate and Global Change, of the University of Graz, Austria. Since 2010 the system is fully operational (Kirchengast et al., 2014). The network consists of 153 meteorological stations in Feldbach (Styria, Austria), which are structured in a grid covering an area of about 20 km × 15 km. Each grid cell masks an area of about 2 km^2. The short distance between the stations (small area for a single grid cell) leads to a very high spatial resolution. A figure of the WegenerNet's grid and stations, shaded with a height map, is given in Fig. IV.1 below.

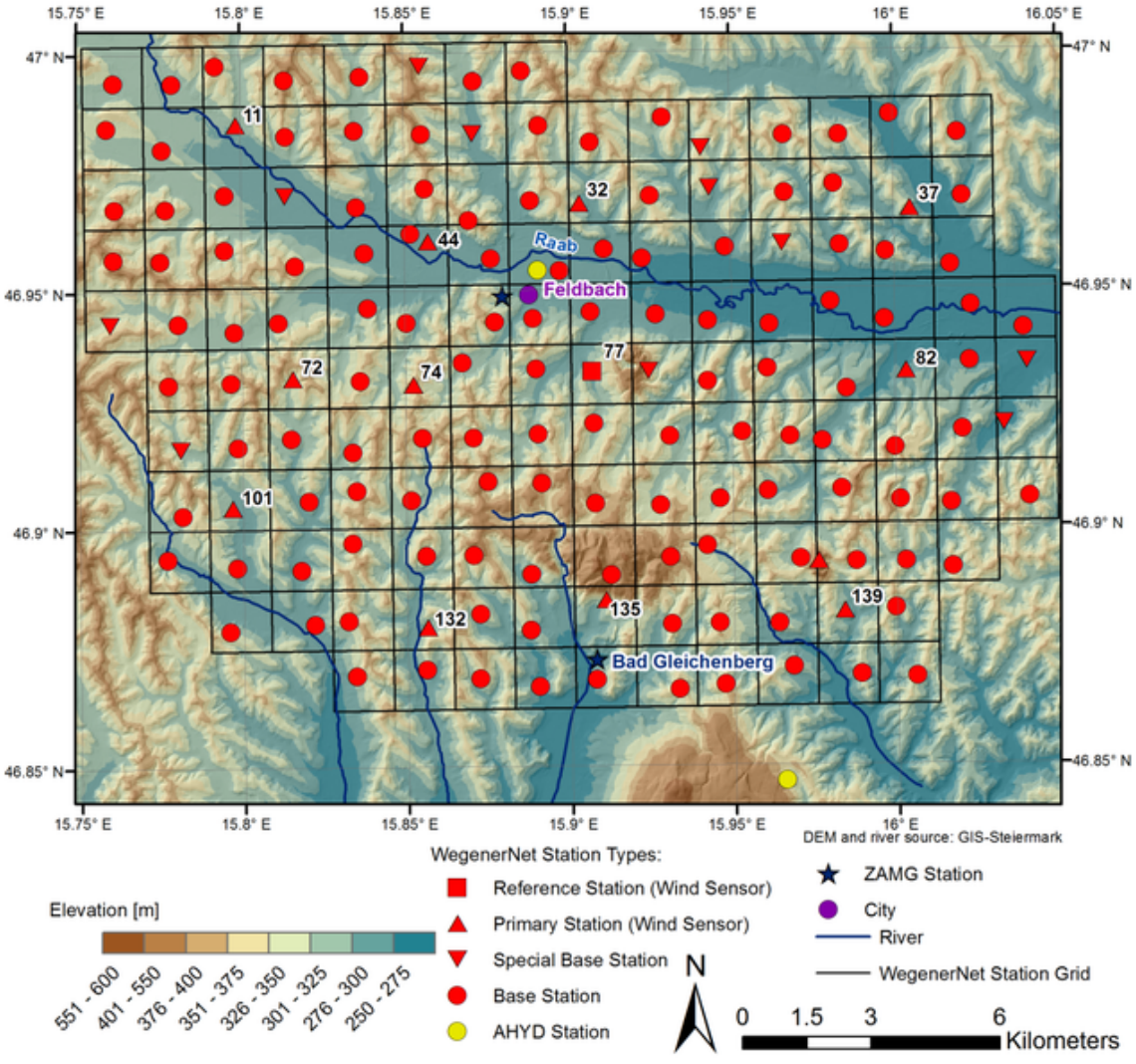

Figure IV.1: GPM-DPR observation principle with the DPR and the GMI[9]

The stations measure meteorological quantities, such as the air temperature, air pressure, precipitation, relative humidity, wind parameters, soil parameters, radiation parameters and hydrological paramters. These

[9]Source: `https://wegcenter.uni-graz.at/de/wegenernet/wegenernet-home/`

observations build the basis of a complete meterological representation of the area.
The following geographical and climatological sketch of the WegenerNet mainly follows the summary in Szeberényi (2014), and the detailed characterisation in Kabas (2012). The WegenerNet is located in the East-Styrian Riedelland (federal state of Styria and Burgenland), which is situated in the southeastern foothills of the Alps. Riedel are long-drawn mountain ridges between two valleys. They show altitudes of up to about 400 m. Therefore, the area is characterised by low hill chains and valley floors. Elevations exceeding the Riedel ridges are remnants of tertiary volcanism (Szeberényi, 2014). The highest point is the Gleichenberger Kogel with 598 m height. The river Raab crosses the WegenerNet from Northwest to the East dividing it into a northern and southern part. The river valley features widths ranging from 800 m to 2500 m. The region lies at the interface between Mediterranean and Alpine climate. Continental climate conditions dominate the area, and consequently, cold winters with occasionally strong winter storms and warm summers occur. Atmospheric inversion and fog is observed frequently, since outflow of cold air pockets is hardly possible. On the ridges the climate is milder with longer sunshine duration in the winter months and lesser frost risk. On the ridges convective precipitation events during summer are more frequent, summer precipitation can emerge in heavy rainfall from thunderstorms. The area is a European hotspot for hailstorms (Kirchengast et al., 2014). The yearly average rainfall is about 800 mm. Due to the landscape orographic rain is at most a minor part of the precipitation, which is important for the comparison to the satellite radar measurements.

The main instrument for precipitation observation is a tipping bucket rain gauge, which is mounted at all stations. However, only twelve of these stations contains a heating and deliver reliable measurements in times of solid precipitation. The principle of a tipping bucket gauge is shown in Fig. IV.2. A funnel collects the water from the rainfall and carries into one of two compartments with a predetermined volume mounted next each other like a seesaw, each compartment representing one of the weights. When the volume of collected water in one compartment reaches the predetermined amount (e.g. 0.1 mm in case of all WegenerNet gauges) the bucket tips, the instrument records this using an electrical contact and drains the collected water. Next, the now heavier other compartment tips, the instrument counts, and releases the water, and so forth. The number of tips are counted and in case of WegenerNet accumulated to five minute samples.

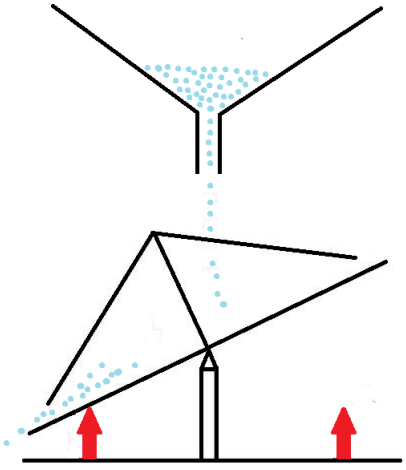

Figure IV.2: Principle of a tipping bucket rain gauge instrument as it is used in the WegenerNet

1 Data

Level 0 data of the WegenerNet are the raw observations carried out by each station in the network. These are transformed to Level 1 data by the WegenerNet Processing System. These Level 1 data have a latency of around 1.5 hours and are checked for their quality and integrity. The Data Product Generator uses Level 1 data to determine the user data, which is then published as Level 2 data. These data include a time series of the measured meterological quantity per station and a 200 m $\times$ 200 m grid. The grid, which is mainly employed in this work as a reference to the GPM-DPR estimates, is determined by a inverse-distance-weighted interpolated method, missing data are filled in by temporal and spatial interpolation (O, 2017). Within two hours, the Level 2 data are published. More information on the WEGN data processing system and data products can be found in Kirchengast et al. (2014), a detailed description is given in Kabas (2012). The data is published in 5-minute accumulations as basic product (basis data). Further products include half-hourly, hourly and daily samples for weather considerations. Climate related data are given in monthly, seasonal, yearly and meteorological-yearly timescales. WegenerNet data are available at the WegenerNet data portal `http://www.wegenernet.org/` in NetCDF format.

Part V

The Paper

The paper was submitted as a discussion paper to the Atmospheric Measurement Techniques Journal (AMT) in October 2018. It is structured in five sections. Section 1 is an introduction, thus repeating the so far described items in short, pointing out the GPM mission and the WegenerNet. Section 2 gives an outline of the data, i.e. rain gauge measurements from the WegenerNet and quantitative precipitation estimates from the GPM-DPR. It is followed by Section 3, which introduces the focus and the methodology of validating GPM-DPR based on a small terrestrial network. Section 4 deals with the results of the validation and its limits. Concluding remarks are pointed out in Sect. 5. In the paper light rain refers to amounts less than 0.5 mm, moderate rain is used for precipitation up to 4 mm and any rainfall greater than 4 mm is denoted as heavy. To give a first glimpse of the data, the distribution of the rainfall amount for all detected events (253 values per measurement technique) is displayed in Fig. V.1. The preciptation that occured has clear peak between 0 mm and 1 mm, thus, the evaluation is biased towards light rainfall.

Figure V.1: Histogram of all data of rainy events collected over the period 2014-2017

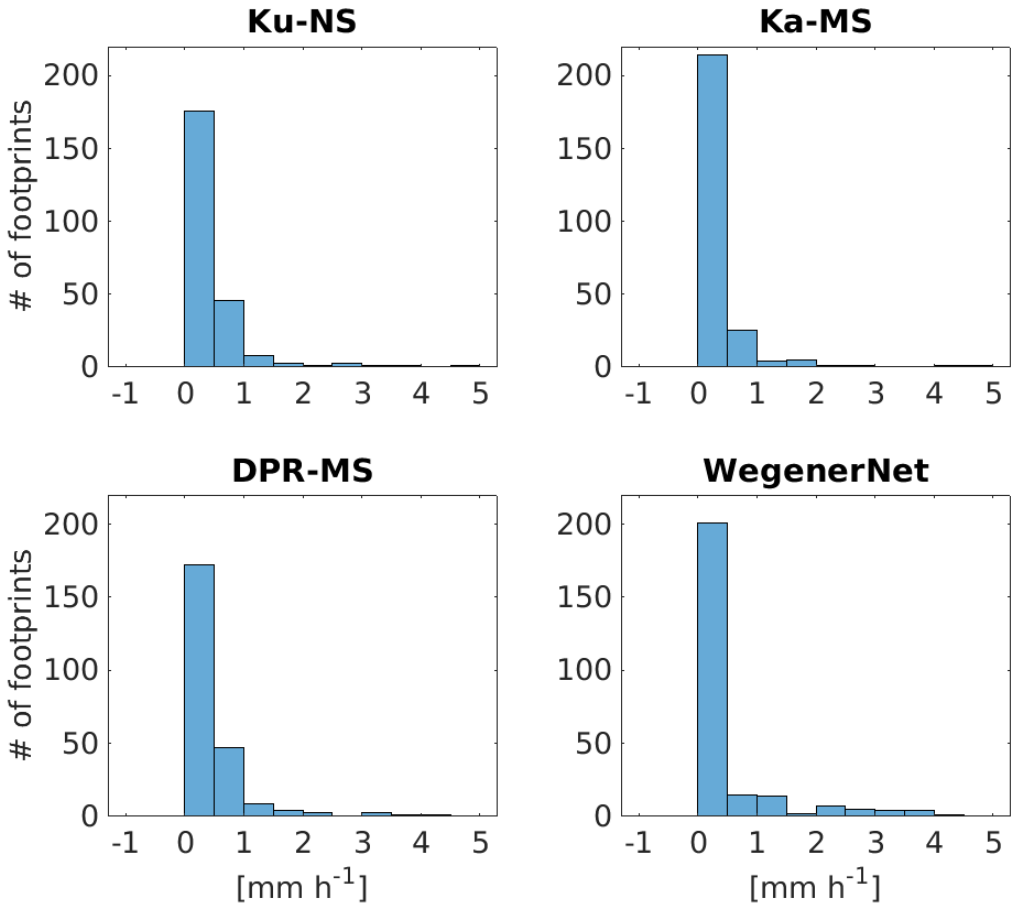

Furthermore, the distribution shows possible disagreements between the radar and the gauges when looking at higher rainfall rates.

Evaluation of GPM-DPR precipitation estimates with WegenerNet gauge data

Martin Lasser[1,*], Sungmin O[1,2,†], and Ulrich Foelsche[1,2,3]

[1]Institute for Geophysics, Astrophysics, and Meteorology/Institute of Physics (IGAM/IP), NAWI Graz, University of Graz, Austria
[2]FWF-DK Climate Change, University of Graz, Austria
[3]Wegener Center for Climate and Global Change (WEGC), University of Graz, Austria
[*]Now at Astronomical Institute, University of Bern, Bern, Switzerland
[†]Now at Biogeochemical Integration, Max Planck Institute for Biogeochemistry, Jena, Germany

Correspondence: Ulrich Foelsche (ulrich.foelsche@uni-graz.at)

Abstract. The core satellite of the Global Precipitation Measurement (GPM) mission provides precipitation observations measured with the Dual frequency Precipitation Radar (DPR). The precipitation can only be estimated from the radar data, and therefore, independent validations using direct precipitation observation on the ground as a true reference need to be performed. Moreover, the quality and the accuracy of the measurements depend on various influencing factors. In this way, a validation may help to minimise those uncertainties. The DPR provides three different radar rain rate estimates for the GPM core satellite: Ku-band-only rain rates, Ka-band-only rain rates and a product combining the two frequencies. This study presents an evaluation of the three GPM-DPR surface precipitation estimates based on the gridded precipitation data of the WegenerNet, a local scale terrestrial network of 153 meteorological stations in southeast Austria.

The validation is based on a graphical and a statistical approach using only data where both Ku- and Ka-band measurements are available. The data delivered from the WegenerNet are gauge-based gridded rainfall observations; the meteorological winter is excluded due to technical reasons. The focus lies on the resemblance of the variability within the whole network and the over- and underestimation of the precipitation through the GPM-DPR. During the last four years 22 rainfall events were observed by the GPM-DPR over the WegenerNet and the analysis rests upon these rainfall events. The WegenerNet provides a large number of gauges within each GPM-DPR footprint. Its biases are well studied and corrected, thus, it can be taken as a robust ground reference. This work also includes considerations on the limits of such comparisons between small terrestrial networks with a high density of stations and precipitation observations from a satellite.

Our results show that the GPM-DPR estimates basically match with the WegenerNet measurements, but absolute quantities are biased. The three types of radar estimates deliver similar results, where Ku-band and dual frequency estimates are very close to each other. On a general level, Ka-band precipitation estimates deliver the best results due to the high number of light rainfall events.

1 Introduction

The Global Precipitation Measurement (GPM) mission aims to give consistent and comprehensive information about Earth's global precipitation. The mission is led by the National Aeronautics and Space Administration (NASA) and the Japan Aerospace and Exploration Agency (JAXA). It is the successor mission of the Tropical Rainfall Measurement Mission (TRMM) and targets to provide advanced information on rain and snow characteristics from multi-satellites. It measures fundamental quantities of the global water cycle, such as the precipitation amount, on a global level. The results are utilised in weather forecasts, flood predictions and river managements, studies on global change and climate variations as well as the assessment of the global water cycle (see JAXA, 2017)

The GPM Core Observatory (GPM-CO) satellite is equipped with an active Dual frequency Precipitation Radar (DPR) and a passive microwave imager (GPM microwave imager - GMI). Together with a constellation of partner satellites from international space and weather agencies, such as the National Oceanic and Atmospheric Administration (NOAA), the Centre national d'études spatiales (CNES) and the Indian Space Research Organisation (ISRO) or the European Organisation for the Exploitation of Meteorological Satellites (EUMETSAT), it provides global-scale precipitation data. The GPM-CO satellite was launched in 2014 and flies at an altitude of 407 kilometers in a non-Sun-synchronous orbit that covers the Earth from 65°S to 65°N. Next to its own measurements, it serves as a reference for unifying the data from the partner satellites (Skofronick-Jackson et al., 2016). The main instrument is in principle a weather surveillance radar operating on two frequencies to map weather events across its swath. The two frequencies allow to estimate the sizes of precipitation particles and detect a wider range of precipitation rates. The microwave imagers augment the core satellite and enable a high temporal resolution for global precipitation maps.

In this study solely the surface rain rate estimates derived from DPR on board the GPM-CO are evaluated and compared to the rain-gauge-based gridded data from the WegenerNet. The WegenerNet is a local scale dense terrestrial network of meteorological stations in the Feldbach region of southeast Austria. It consists of 153 meteorological stations, constructed in an area of roughly 20 km x 15 km, forming a structured grid with a cell area for each station of about 2 km^2 (see Fig. 1). The orography and vegetation has no significant influence on the accuracy of the rain gauge measurements. Each station measures meteorological quantities such as temperature, humidity and precipitation (see Kirchengast et al. (2014) for further details). In all stations a tipping bucket rain gauge instrument with a volume of 0.1 mm is used, however, only twelve contain a heating device, and are, therefore, able to reliably measure winter precipitation.

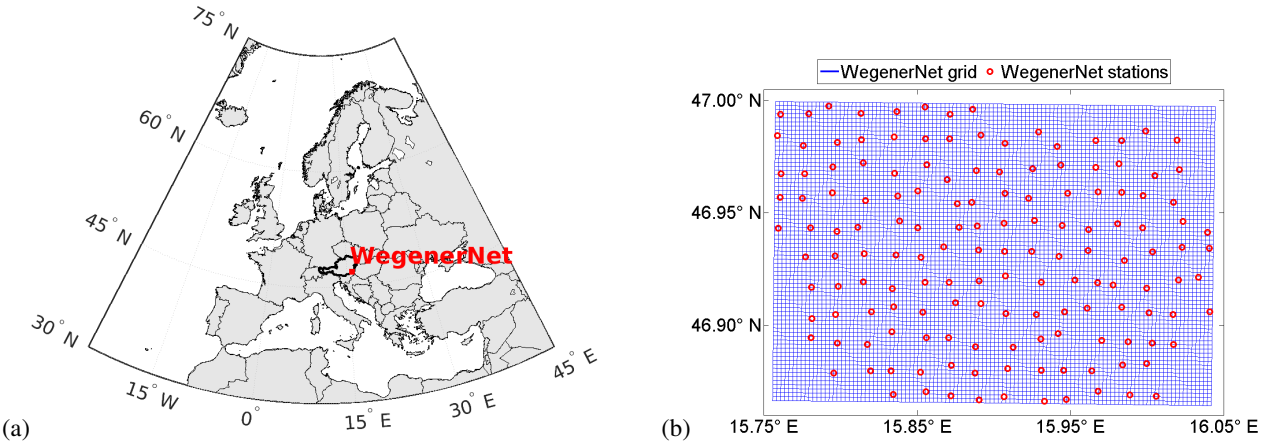

Figure 1.

(a) Location of the WegenerNet in Europe.

(b) Geometry of the WegenerNet; red circles indicate the meteorological stations, blue displays the 200 m grid; the area is roughly 20 km × 15 km. Measurements are taken in five minute accumulations.

Gauge data as ground reference are widely used in many existing validation studies (e.g. Amitai et al., 2015; Tan et al., 2017; O et al., 2017). Since satellite estimates provide only measurements at points in time and not accumulations, one prerequisite for evaluating with terrestrial gauge data is that the accumulations are as short as possible, but still providing high quality information. Even though the WegenerNet is of very small scale, it provides in its 5 minutes accumulations considerably more and better of information, especially because of the high spatial resolution in the covered area. Additionally, the biases of the network are known and corrected (see O et al., 2018). Therefore, it is possible to evaluate every DPR footprint based on the information of 8-10 or even more stations. The drawback is the small number of fly-overs with actual precipitation, which allows only for an event-based analysis.

The paper is structured in four upcoming sections. Section 2 gives a description of the data, i.e. rain gauge measurements from the WegenerNet and quantitative precipitation estimates from the GPM-DPR. It is followed by Section 3, which introduces the focus and the methodology of validating GPM-DPR based on a small terrestrial network. Section 4 deals with the results of the validation and its limits. Finally, concluding remarks are pointed out in Sect. 5.

2 Data

2.1 WegenerNet

The WegenerNet is a network of high spatial resolution for weather and climate studies, located in the Feldbach region in southeast Austria. The region is characterised by moderate hilly landscape in the alpine foreland with altitudes between 260 m to 600 m, and the valley of the river Raab. The network incorporates 153 weather stations in an area of about 300 km^2, employing tipping-bucket gauges to collect rainfall measurement data every 5 min. The general user data products are station time series, as well as a 200 m × 200 m gridded data set, calculated by applying an inverse-distance-weighted interpolated method. The data products are available online at the WegenerNet web portal (http://www.wegenernet.org/) within 2 h latency.

The WegenerNet provides a robust ground reference, its data bias is well studied (O et al., 2018), and it has been used in several other studies for satellite data validation (e.g. O et al., 2017; Kidd et al., 2017). Furthermore, the spatial uncertainties of rainfall over the WegenerNet were investigated by O and Foelsche (2018). More information on the WegenerNet and its data products can be found in Kirchengast et al. (2014). The tipping bucket rain gauge instruments collect water up to 0.1 mm, which is the minimum resolution of the WegenerNet precipitation measurements. Since only a small number of stations are heated, times with possibly solid precipitation are excluded from the evaluation (the meteorological winter, i.e. Dec. 1$^{\mathrm{st}}$ to the end of February). The data from the tipping-bucket gauges are accumulated to five minute samples, which is the basic data product of the WegenerNet. Thus, the basic data are a sum of measurements that refers to an interval in time (in contrast to the GPM-DPR estimates, which refer to a point in time). Further products include half hour samples, one hour samples, daily, monthly, seasonal and yearly data.

The high spatial resolution of the WegenerNet allows an investigation of each footprint based on multiple gauges. However, due to its small extent and due to the low sampling frequency of GPM, the number of rainfall data samples is limited.

The minimum resolution, which is also roughly the precision, of the WegenerNet is twice as good as the GPM-DPR estimates' minimum resolution. However, there is no other precision (quality) information for the GPM-DPR estimates. Even though the uncertainties are only better by the factor of two, the WegenerNet provides accurate information, not only whether precipitation occurred but also on the amount of rain. Furthermore, it delivers reliable (clear precision information given) measurements over all amounts of rain. The gridded precipitation and the station-wise precipitation reflect the same information (see Fig. A1 and A2 in the appendix). For the evaluation mainly the gridded gauge data were taken into account because of their higher resolution, and therefore, more information on extensive parts of the WegenerNet (such as the area covered by one footprint of the satellite's radar).

2.2 GPM-DPR

The GPM-DPR provides accurate rain rate estimations on a global level. The DPR radar instrument measures on two different channels (Ka-band at 35.5 GHz and Ku-band at 13.6 GHz) to obtain the three-dimensional structure of precipitation, including heavy (tropical) rainfall and light rainfall at mid-latitudes.

In general, the strength of the radar echoes is affected by attenuation due to precipitation. The amount of attenuation depends

on the frequency and the size of raindrops. The precipitation radar matches the transmission pulse timings and the radar beam position with the attenuated echo to estimate the size of a raindrop (see JAXA, 2017). The GPM-DPR uses differential attenuation between the Ku-band and the Ka-band frequencies and the Variable Pulse Repetition Frequency (VPRF) technique for high resolution rain rate estimates. The amount of rain is obtained in further processing based on various algorithms (see Iguchi et al., 2015). The Ku-band precipitation radar (KuPR) has an observation swath of 245 km with 49 bins (Normal Scan - NS), each resulting in a circular footprint of 5.2 km diameter. The bins do not overlap. The KuPR is more sensitive to heavy and moderate rainfall. The KaPR on the other hand, has half of the swath size of KuPR with 120 km and 49 bins. 25 bins between KuPR and KaPR are overlapping, i.e. KaPR Matched Scan (MS). KaPR shall provide better information on light rainfall and snow. The second scan, that is provided for the KaPR is a high sensitivity scan with 24 bins, where the beams are interlaced within the scan pattern of the matched beams (Iguchi et al., 2015). The range resolution is 250 m for KuPR and 250m/500m for KaPR. The Dual Frequency (DF) rain rate estimation combines Ka- and Ku-band information to the DPR product. It is available for NS, MS and HS. Where the swaths do not overlap KuPR data are provided in the DPR product (JAXA, 2017).

In order to acquire as many rain rate estimates as possible over the WegenerNet, the NS was taken into account for the Ku-band and the MS for the two other products. The minimum resolution is given by the documents (JAXA, 2017) with 0.2 mm for the Ka-band and the merged product. The Ku-band estimates resolve a minimum 0.5 mm of rainfall. However, recent evaluations assign to the KuPR estimates the same quality as the Ka-band delivers (Tan et al., 2017; Hamada and Takayabu, 2016).

In contrast to the observations taken by the terrestrial stations, the radar measurements resemble only one point in time and are converted through algorithms (e.g. Iguchi et al., 2015) into a rain rate per hour. This, however, implies that the matching between observation time and location of the rainfall is crucial to the quality of the product. Even if the estimated rainfall is correct, it needs to be located on the right spot at the right time.

2.3 Selected data

In order to compare the two kind of data sets, two requirements have to be met: First, the radar observations must cover the area of the terrestrial network and second, precipitation must occur during this short time interval. This reduces the possible events for the evaluation drastically.

To evaluate the GPM-DPR rain rate estimates with the WegenerNet, every event in the DPR data was sought after, where the satellite's swath of all three data types (NS for KuPR and MS for the other two) passes the WegenerNet and rain is detected in at least one of the three GPM-DPR products.

For the study period of four years, this yields to

- 426 visits of the GPM core satellite over the WegenerNet
- with > 4000 footprints.
- 24 events with rain detected and
- a sum of 253 footprints.

5

This gives an average of 10 footprints per fly-over. Each footprint covers approximately 8-12 stations.

If an event contains footprints in which the estimation delivers zero rain rate, this zero is taken into account as actual estimation and tested against the WegenerNet. Since the WegenerNet is of local scale, only up to ten times a month the satellite's ground track crosses the area. With an average of around 800 mm of rain per year, the region of Feldbach, where the WegenerNet is located, is not the most rainiest. Therefore, only 24 events were detected. Two events had to be excluded because of missing WegenerNet gridded gauge data. Table 1 lists the remaining events.

Table 1. Evaluated rainfall events. Note that the four highlighted events are analysed in detail.

	date	avg. rain rate Ku-NS [$\mathrm{mm\,h^{-1}}$]	avg. rain rate Ka-MS [$\mathrm{mm\,h^{-1}}$]	avg. rain rate DPR-MS [$\mathrm{mm\,h^{-1}}$]	avg. precip. WegenerNet [$\mathrm{mm\,h^{-1}}$]
Event 1	2014-04-29	0.26	0.07	0.29	0.05
Event 2	2014-05-17	0.32	0.00	0.17	0.13
Event 3	2014-05-18	0.31	0.12	0.22	0.26
Event 4	2014-06-13	0.00	0.00	0.00	0.00
Event 5	2014-06-24	0.08	0.08	0.00	0.26
Event 6	2014-07-02	-	0.00	-	0.00
Event 7	**2014-07-10**	**0.28**	**0.12**	**0.29**	**0.30**
Event 8	2014-07-10	0.02	0.00	0.04	0.00
Event 9	**2014-08-05**	**0.43**	**0.26**	**0.42**	**0.14**
Event 10	2014-08-13	0.11	0.04	0.15	0.00
Event 11	2014-10-21	0.09	0.06	0.10	0.01
Event 12	**2014-10-22**	**0.71**	**0.45**	**0.82**	**2.82**
Event 13	2015-06-15	0.06	0.05	0.06	0.00
Event 14	2015-08-15	0.44	0.19	0.64	0.14
Event 15	2015-10-10	0.40	0.07	0.43	0.93
Event 16	**2016-05-02**	**2.02**	**2.37**	**2.16**	**2.43**
Event 17	2016-06-19	0.39	0.24	0.40	0.41
Event 18	2016-06-27	0.46	0.22	0.48	0.09
Event 19	2016-07-16	0.75	0.39	0.76	0.05
Event 20	2017-05-15	0.21	0.06	0.27	0.15
Event 21	2017-05-15	0.00	0.00	0.58	0.00
Event 22	2017-08-28	0.00	0.00	0.00	0.00
Average	-	0.35	0.22	0.39	0.37

6

Within those events three events provide zero rain in WegenerNet and radar estimates (Events no. 4, 6, 22). These events are included because there was rain slightly outside of the WegenerNet observed by the satellite and the "zero rain" information gives an actual information that can be evaluated with the WegenerNet. Event no. 21 had to be omitted because of only one footprint partly covering the Southwest border of the WegenerNet in the MS. The NS (Ku-band) covered the whole network, however, no rain was detected. Generally, the events show very light rain, only two of them have an average of more than 1 $\mathrm{mm\,h^{-1}}$. The events in bold lettering are analysed in more detail; two with light rainfall (no. 7 and 9) and two with heavier rain (no. 12 and no. 16). Since GPM estimates are given in the unit of [$\mathrm{mm\,h^{-1}}$], the WegenerNet data are converted from millimeter per 5 minutes to millimeter per hour.

The data can be easily visualised (see Fig. 2 for Event no. 16). Note that the circular footprint is distorted into an ellipse due to the meridian convergence.

The GPM-DPR estimates provide one rain rate per footprint and the footprints do not overlap. In contrast to that, the WegenerNet has about 8 to 10 stations per footprint and one cell of the gridded rain gauges covers roughly an area of 200 m x 200 m, which sums up to around 500 grid box values per footprint. As one can see in Fig. 2, every footprint contains a large range of rainfall and a lot of variability. All of these shall be approximated by one single value the GPM-DPR delivers. For the comparison in this study, the average of the gridded data within the footprint is taken as the most representative value for the WegenerNet and in a least squares sense it is the best estimation. The kind reader may keep in mind, that the GPM-DPR footprint rain rate estimates are treated as mean areal rainfall, thus also averaging intra-footprint rainfall. The DPR misses spatial information of highly variable rainfall events (inter-pixel rainfall variability) within a certain area (see bottom-right plot in Fig. 2). The fact, that the WegenerNet captures this inter-pixel rainfall variability and intra-footprint rainfall variability (bottom-left graph of Fig. 2), makes it a robust ground reference. The most important statistical measures on the WegenerNet for 2$^{\mathrm{nd}}$ of May, 2016 are provided in Table 2. During this event the areas outside of the footprints showed a similar behaviour as inside and as the whole network, but this is not necessarily the case for strong convective events.

Table 2. Statistical properties for the WegenerNet on 2$^{\mathrm{nd}}$ of May, 2016 (Event 16)

	whole WegenerNet	inside footprints	outside footprints
Mean [$\mathrm{mmh^{-1}}$]	2.34	2.41	2.25
Standard deviation [$\mathrm{mmh^{-1}}$]	1.12	1.14	1.08
Normalised standard deviation [%]	48	47	48

The large normalised standard deviation implies big variations within the whole area.

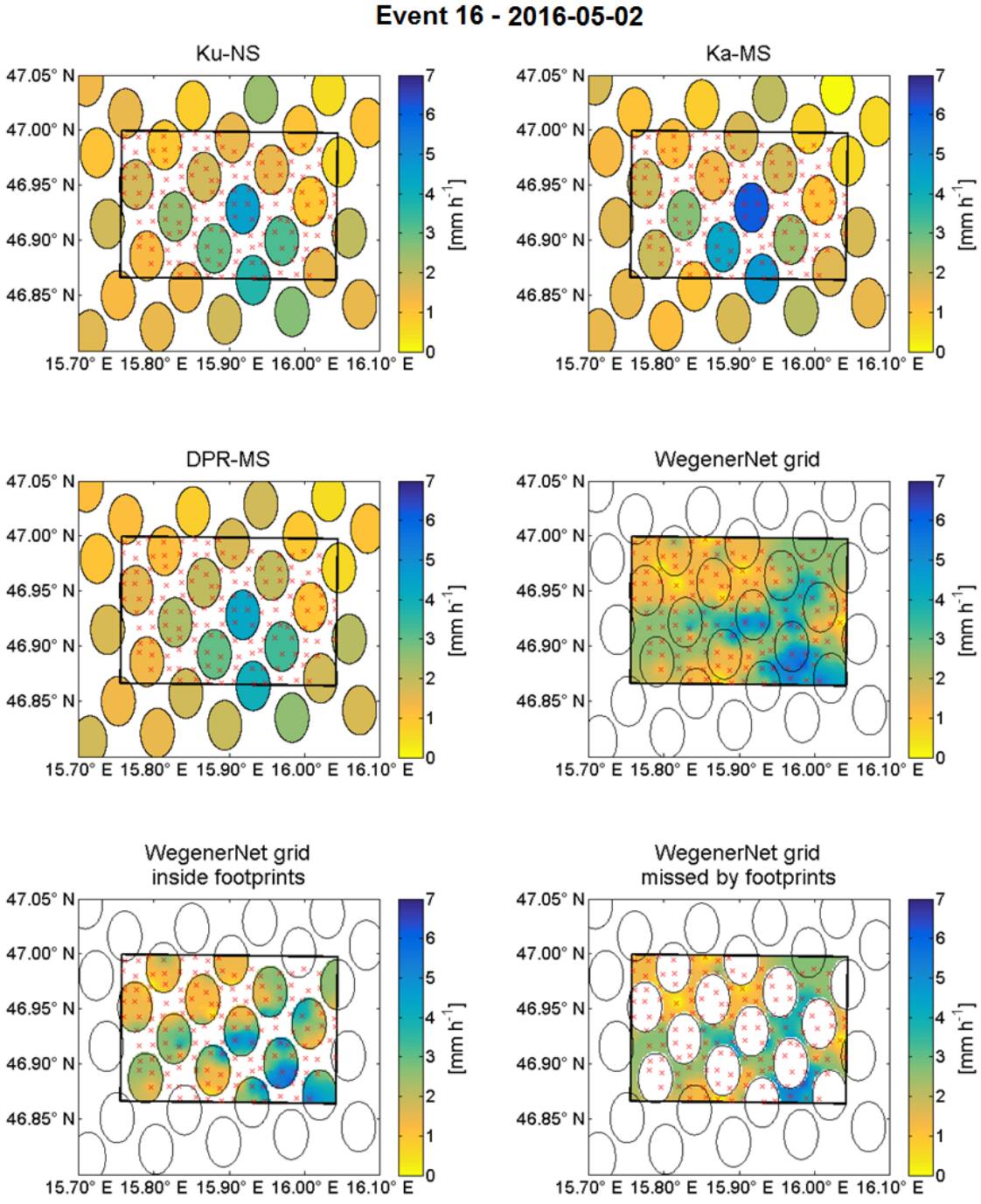

Figure 2. Measurements from the GPM-core satellite (Ku-NS, Ka-MS, DPR-MS) in and around the WegenerNet compared to WegenerNet grid data for the 2nd of May, 2016 including what is detected by the satellite and what is missed (lower graphs).

8

3 Methodology

The evaluation in this study is based on an interpretation of 22 events using graphical support (such as scatter plots) and mathematical tools: We adopt a correlation and a bias between the GPM-DPR and the WegenerNet and statistics based on a contingency table. The statistical items are the Proportion Correct (PC), the Frequency Bias Index (FBI), the Probability Of Detection (POD), the False Alarm Ratio (FAR) and the Probability Of False Detection (POFD). The events are not interrelated, no time series analysis can be applied. Therefore, the interpretation is event-based.

The GPM-DPR delivers one rain rate value per footprint. These footprints are mapped to the WegenerNet gridded gauge data. All grid cells inside one circular footprint and the grid cells that are intersected by the footprint's border are accounted as the WegenerNet's equivalent to the footprint. As the WegenerNet observes multiple gauges per footprint, the arithmetic mean is taken as most representative value. Even if the gauge observations within the footprint do not follow a Gaussian distribution, the mean value delivers a clear message about the regarded area.

In the following equations, G denotes the GPM-DPR estimates and W the WegenerNet. The correlation used is the Pearson's correlation coefficient, Eq. (1).

$$r = \frac{\sum_{i=1}^{n}(G_i - G_{\mathrm{mean}})(W_i - W_{\mathrm{mean}})}{\sqrt{\sum_{i=1}^{n}(G_i - G_{\mathrm{mean}})^2 \cdot \sum_{i=1}^{n}(W_i - W_{\mathrm{mean}})^2}} \tag{1}$$

The bias is calculated as the average of the deviation between the GPM-DPR estimates and the WegenerNet. It is not normalized with W_{mean} because of the light rainfall events, which would lead to a huge bias in case of a very small mean.

$$b = \frac{\sum_{i=1}^{n} G_i - W_i}{n} \tag{2}$$

For the contingency table, the estimates are compared to the ground reference and divided into four groups:

- Hits: Both systems provide precipitation information.
- False alarms: Only the GPM-DPR shows rain.
- Misses: The GPM-DPR does not deliver rain, whereas the WegenerNet does.
- Correct negatives: Both systems give no rain.

From the amount of these values, statistical items can be derived. The kind reader may note, that the number of correct negatives can easily take an effect on the results. Thus, the events to evaluate have to be carefully chosen.

The proportion correct (PC, Eq. 3) is the number of hits plus the number of correct negatives divided by the whole sample size (n), thus, providing an information about the number of correctly detected events. It ranges between 0 and 1 with a perfect score of one (i.e. 100% of the events show the same type of information between the GPM-DPR and the WegenerNet).

$$PC = \frac{N_{\mathrm{hits}} + N_{\mathrm{correct\ negatives}}}{n}. \tag{3}$$

The FBI (Eq. 4) gives an impression whether an over- or an underestimation occurs. It describes the ratio between the number of footprints that are detected by the GPM-DPR to feature precipitation and the number of footprints that show precipitation according to the WegenerNet. Its range is between 0 and ∞, with an perfect score of 1. An FBI larger than 1 means overestimation, <1 is an underestimation.

$$FBI = \frac{N_{\text{hits}} + N_{\text{false alarms}}}{N_{\text{hits}} + N_{\text{misses}}}. \tag{4}$$

The probability of detection (POD) is

$$POD = \frac{N_{\text{hits}}}{N_{\text{hits}} + N_{\text{misses}}}, \tag{5}$$

The POD ranges from 0 to 1, with one as all rain events detected correctly (no miss). It is only sensitive to missed events, this means, it can be (artificially) improved by overestimation, which leads to a reduction of misses. The increase of false alarms does not influence the POD. For a more sophisticated interpretation, the constraint of the GPM-DPR estimates being in an interval of $W_{\text{mean}} \pm W_{\text{std.}-\text{dev.}}$ is applied to the POD.

The FAR is taken into account to cross-check with the POD (Eq. 6).

$$FAR = \frac{N_{\text{false alarms}}}{N_{\text{hits}} + N_{\text{false alarms}}}. \tag{6}$$

Again the range is between 0 and 1, with 0 as perfect score, which means that there is no event, where the GPM-DPR sees rain and the WegenerNet does not. The FAR is not sensitive to misses, but to false alarms. Therefore, it can be improved by underestimation (reducing the possible amount of false alarms, but also increasing the possible amount of misses). POD and FAR together provide a robust information on the quality of the estimation.

Finally, the POFD is calculated as

$$POFD = \frac{N_{\text{false alarms}}}{N_{\text{false alarms}} + N_{\text{correct}-\text{negatives}}}. \tag{7}$$

It ranges between 0 and 1, where 0 is the perfect score. In contrast to the FAR the POFD takes the correct negatives into account, which may lead to a very low value. Underestimation improves the POFD.

4 Results

4.1 Evaluation of all rainfall events

The most basic evaluation is the series of footprints for all events (Fig. 3). Note that this is not a time series in the sense that any time series analysis can be applied (no uniformly spacing etc.), but still it is ordered in time. At a first glance, the GPM-DPR estimates resemble the WegenerNet quite well. Over- and underestimations as in Event no. 12, 16 and 19 happen, but the general structure can be seen in the satellite data. Even when the GPM-DPR estimates over- or underestimate the true precipitation, more than 70% of the GPM-DPR precipitation rates are within the range of the respective WegenerNet gauges

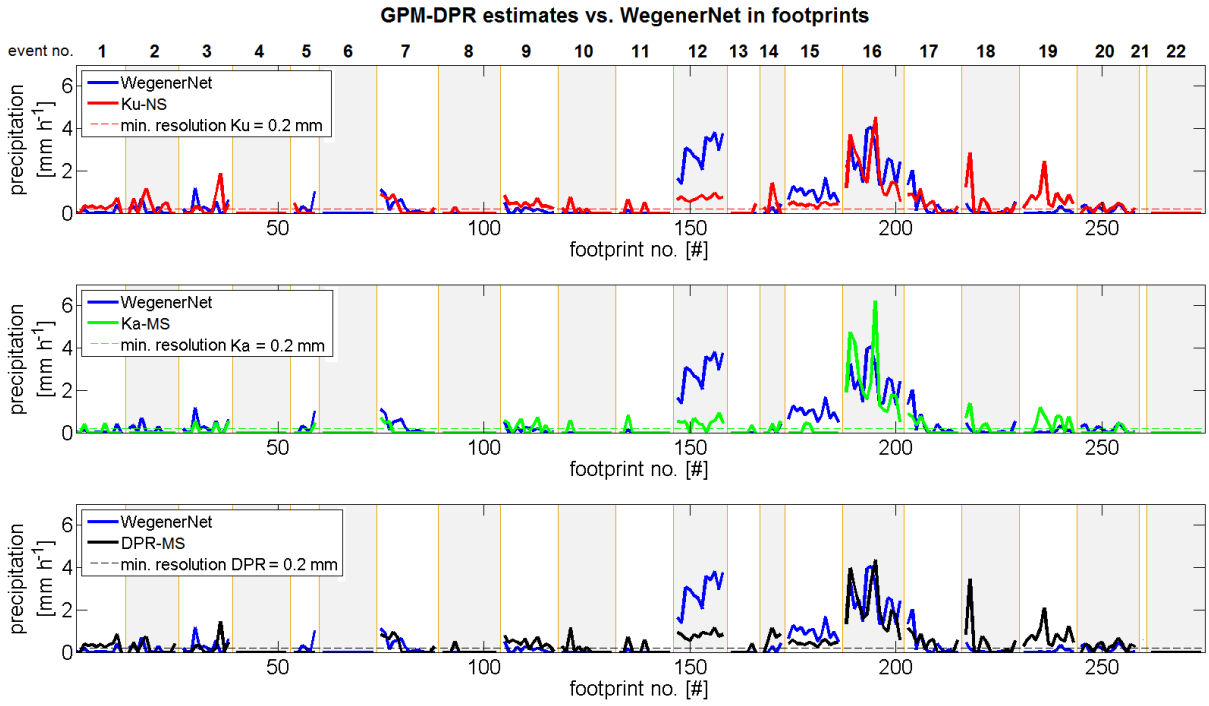

Figure 3. GPM-CO estimates over the WegenerNet (average of WegenerNet 5-min accumulation in the respective footprint) in the years 2014-2017, only events with precipitation detected in either Ku-NS, Ka-MS or DPR-MS were taken into account. The meteorological winter (Dec. 1st to the end of February) is excluded. Each box shows precipitation at a same time (one event per box) but different locations.

inside the footprint (for KaPR it is more than 90%) and almost 60% fulfill the tighter restriction of lying within one time the standard deviation around the average (73% for KaPR). See Fig. A3 in the appendix for a graphical representation.

Testing the GPM-DPR estimates directly against the WegenerNet precipitation leads to a scatter plot (Fig. 4). It shows, that the DPR tends to underestimate the WegenerNet gauges, as more estimations can be found below the diagonal. A point of interest is when one system provides the information of zero rain and the other detects precipitation, which is basically a mis-detection if the WegenerNet does not see rainfall. However, since the mean of the gridded gauge data inside the footprint is taken into account, close to zero rainfall (rounded to zero) inside the footprint does not mean that no precipitation occurred. GPM-DPR probably observed a part of the WegenerNet grid boxes in its footprint area, where there was no rainfall, even though it rained in the other part of the WegenerNet grid boxes. This over-/underestimation of satellite precipitation estimates due to the subpixel-scale rainfall variability was also found by O et al. (2017). Therefore, the detection of rain in the GPM-DPR cannot be treated as completely wrong without considering a certain interval around the mean (range inside the footprint and/or the standard deviation of the mean).

The most general statistics can be applied by setting up a contingency table and counting the number of hits, misses, false

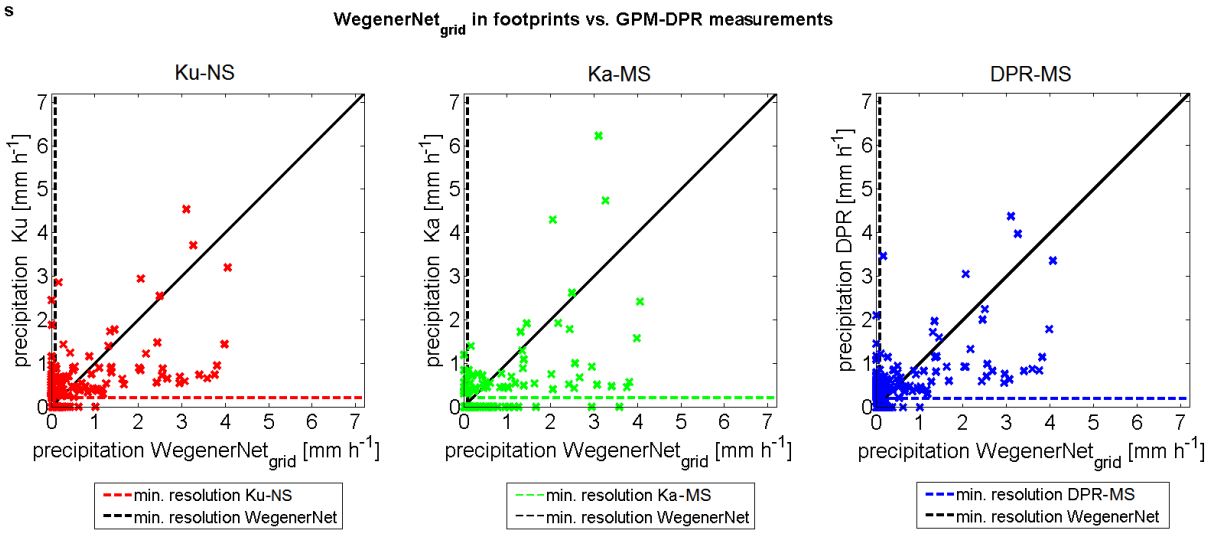

Figure 4. Average of GPM-DPR observations as a function of WegenerNet measurements inside the resp. footprints. The diagonal denotes the line where the satellite measures the same as the terrestrial network.

alarms and correct negatives (Table 3). The ground reference provides 126 times of precipitation inside a footprint and 127 times there was no rain detected. The Ku-NS product and the DPR-MS always score the same number, and are in lead when it comes to actual hits. The Ka-MS misses more than twice as much as the Ku-NS and hits only 2/3 of the KuPR, however it is more sensitive to delivering correct negatives. Furthermore, only five false alarms are given by KaPR. Even though the KaPR scores as many hits as misses, it performs quite well due to its ability of correctly mirroring the WegenerNet's non precipitation events (few false alarms, lots of correct negatives). The PC, FBI, POD, FAR and POFD are items derived from the contingency table. These are given in Table 4. The PC is around 0.70 for all three products, which means that around 70% of all footprints correctly detect rain/no-rain. However, this number may be misleading, because the no-rain footprints get the same weight as the ones with rain. Therefore, a lot of no-rain events, correctly detected, increase the PC. In our case, the number of rainy footprints is almost equal to the number of no-rain footprints, hence, it can be assumed that 70% is a good rate.

Table 4. Statistics derived from the contingency table for all events.

	Ku-NS	Ka-MS	DPR-MS
PC	0.70	0.72	0.70
FBI	1.10	0.52	1.10
POD	0.75	0.48	0.75
FAR	0.32	0.08	0.32
POFD	0.35	0.04	0.35

Table 3. Contingency table

	WegenerNet →	yes	no	Σ
↓ GPM-DPR				
yes	Ku-NS	**hits** 95	**false alarms** 44	139
	Ka-MS	60	5	65
	DPR-MS	95	44	139
no	Ku-NS	**misses** 31	**correct negatives** 83	114
	Ka-MS	66	122	88
	DPR-MS	31	83	114
Σ	Ku-NS	126	127	253
	Ka-MS	126	127	253
	DPR-MS	126	127	253

The FBI gives an impression about the under- or overestimation of the precipitation for a certain number of events. It does not take into account whether a single footprint was subject to mis-estimation or not. The correct negatives do not influence the FBI. The Ku-NS and the DPR-MS tend to overestimate (FBI = 1.10; more yes events in the KuPR than in the ground reference), whereas the KaPR underestimates the precipitation (FBI = 0.52).

The POD has a value of 0.75 for Ku and DPR-merged and 0.48 for the Ka-band. The better performance of the Ku-band results may be assigned to the fact that a lot of "correct negatives", i.e. both systems see zero rainfall, occur and these do not contribute to the POD. The probability of detection in each event, however, shows more discrepancies for the POD (see Table A1). According to Skofronick-Jackson et al. (2016) the POD on a global level is >64%, which shows that the GPM-DPR is suited to capture the precipitation that takes place over the WegenerNet. The good POD of Ku-NS and DPR-MS is supported by the FBI, which shows a tendency to overestimation. Since the POD can be increased by overestimation (false alarms do not contribute to the POD), the FAR is considered as well. It shows that the rate is around 30% for Ku-NS and DPR-MS, whereas the KaPR has a FAR of only 8%, thus, delivering very few false alarms. The FAR can be improved by underestimation, which closes the circle to the FBI. The overestimation in Ku-NS and DPR-MS worsens the FAR, but enhances the POD, the underestimation through KaPR improves the FAR. Since the POD and the FAR do not consider the number of correct negatives, the POFD sheds light on the probability of getting a false alarm compared to the correct negatives. Here, the KaPR and its tendency to underestimation (few false alarms), delivers best results.

Very low rainfall events are better detected by the Ka-band frequency, whereas heavier rainfall can be seen in Ku (as expected) and Ka. The dual frequency product is in between Ku-NS and Ka-MS with a tendency of giving more weight to Ku-band than Ka-band data. The events without rainfall over the WegenerNet are detected with a 100% score in all products.

Considering the constraint that the GPM-DPR estimates must be in an interval of ± standard deviation around the mean of the WegenerNet in the respective footprint, the POD for the series of events gives around 50% for the GPM-DPR estimates (see Table 5, bottom). This is an increase for the KaPR estimates, a decrease for the other two. The constraint adds a lot of misses to the statistics for Ku-NS and DPR-MS, while decreasing the number of hits. For the Ka-band estimates, this improves the statistical result slightly (PC = 0.74%, FBI = 0.56). For the Ku-NS and DPR-MS rain rate estimates the FBI decreases towards underestimation, while the FAR gets worse (less hits shrinks the FBI and increases the FAR). The PC drops to less than 60%. Since the POFD keeps its level, the number of false alarms is stable.

Table 5. Contingency table and statistics with the constraint that a hit is only scored when the GPM-DPR estimate is within the interval of $[W_{\text{mean}} - W_{\text{std.-dev.}}, W_{\text{mean}} + W_{\text{std.-dev.}}]$.

	WegenerNet →	yes	no	Σ
↓ GPM-DPR				
yes	Ku-NS	**hits** 65	**false alarms** 44	109
	Ka-MS	65	5	70
	DPR-MS	67	44	111
no	Ku-NS	**misses** 61	**correct negatives** 83	144
	Ka-MS	61	122	183
	DPR-MS	59	83	142
Σ	Ku-NS	126	127	253
	Ka-MS	126	127	253
	DPR-MS	126	127	253

	Ku-NS	Ka-MS	DPR-MS
PC	0.58	0.74	0.59
FBI	0.87	0.56	0.88
POD	0.52	0.52	0.53
FAR	0.40	0.07	0.40
POFD	0.35	0.04	0.35

The (counter-intuitive) improvement of the performance of Ka-band rain rate estimates when constraining, can be explained with very light rainfall events, where a Ka-band miss lies within the constraining range, and is consequently detected as a hit. In

a more balanced testing environment with more events of heavier rain, the KuPR would catch up. Notable is the DPR-MS estimation which is closer to the Ku-band estimates, even though both frequencies are combined. The influence of the constraint on the performance is very distinct in Event 12, where the simple POD gives values between 0.83 and 1 and the constrained version discards them.

The series of footprints of all events and the correlation and bias within one event is displayed in Fig. 5. There are no clear characteristics which GPM-DPR product catches the precipitation variations inside the WegenerNet better. Some events, e.g. no. 12, are not correlated. There is no event anti-correlated, which shows that the GPM-DPR estimates for one event are not completely shifted compared to the WegenerNet variations. The mean of the correlations over all footprints is $r = 0.42$ for Ku-NS and $r = 0.47$ for Ka-MS and DPR-MS.

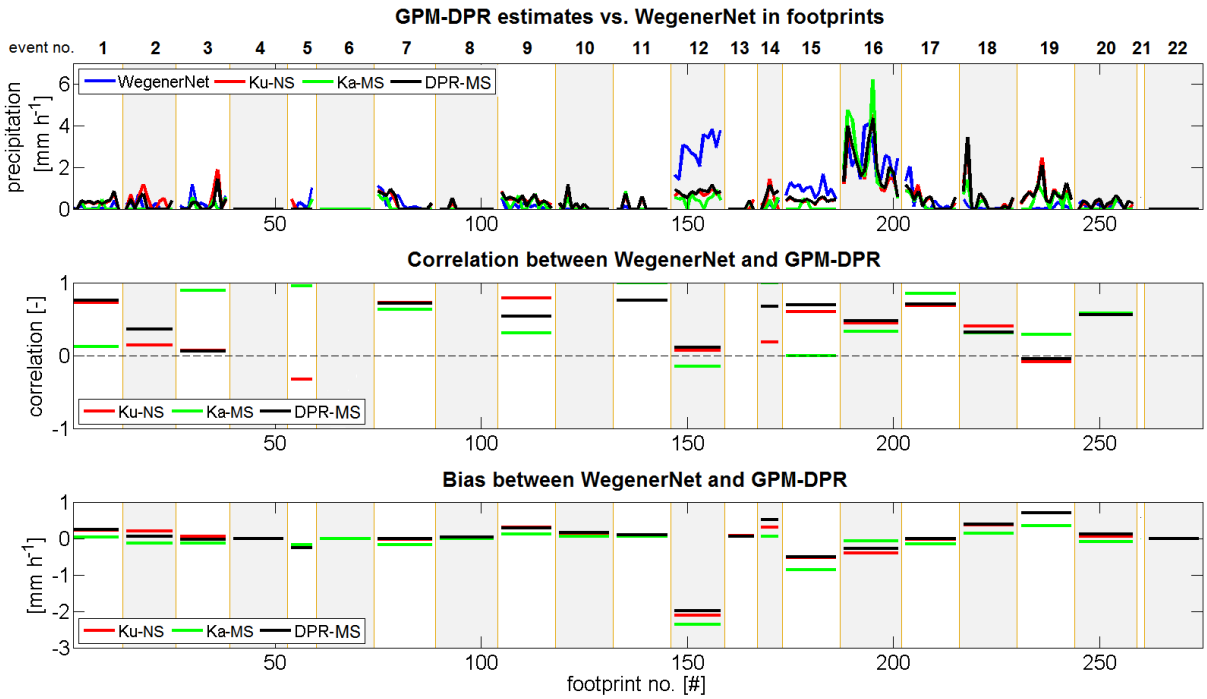

Figure 5. Correlation and bias between GPM estimates and the WegenerNet within all detected events. The topmost graph gives the precipitation of the events again.

Even though the bias can be high, there is no connection to the correlation. Perfect bias of zero occurs only at events without precipitation. Considering the bias and the correlation, one can derive, that the DPR-MS is closer to Ku-NS than to Ka-MS. Ka-band estimates have in general a lower bias than the others, this again may be explained with the high number of light rainfall events.

4.2 Analysis of example rainfall events

The example events where chosen based on the amount of rainfall in the WegenerNet. Two with light rain (no. 7 and 9) and two with moderate to heavy rain up to 7 $\mathrm{mm\,h^{-1}}$ in a certain footprint (no. 12 and 16). According to the rain type specified by the GPM-DPR data, all events are a stratiform phenomena, when Ku- or Ka-band data are considered, however dual frequency estimates state mostly convective rainfall. A look at WegenerNet reveals that the light rain events are more of a convective nature and the other two show stratiform behaviour. The events with light precipitation are in the hot season (July and August), the other ones in spring and autumn.

The first event to investigate is Event no. 7 on 10th of July, 2014, where the GPM-CO passed the WegenerNet at 11:40 and detected light precipitation. The chronological order of the footprints (each box depicts one footprint) and the estimated amount of precipitation is given in Fig. 6, the upper part showing the GPM-DPR estimates and the gauge station precipitation from the WegenerNet and the lower graph depicting the gridded gauge data instead of station data.

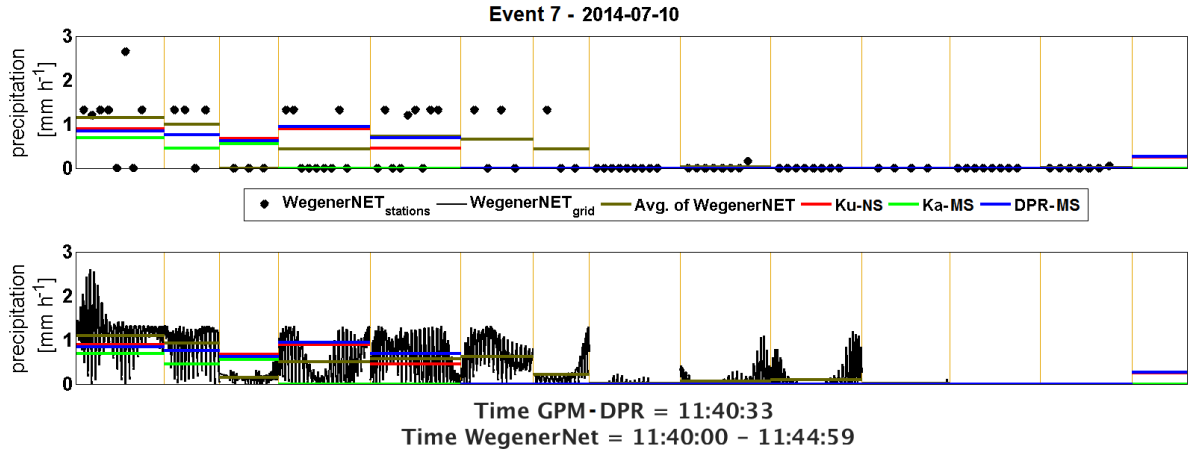

Figure 6. Series of footprints for Event 7 (10th of July, 2014) compared to station and grid data.

More than half of the footprints do not feature any rain, which is correctly detected by the radar estimates. Within the other footprints, especially the ones in the middle of the graph, some information is added in the gridded gauge data compared to station alone because not only the gauges inside the footprint are used for the grid generation. All radar estimates are within the range of the respective WegenerNet footprint and close to the mean of the gauges. Thus a small bias is expected. The correlation between the terrestrial and the satellite data is close to one, which emphasises the quality of this event (see Event no. 7 in Fig. 5). The proportion between over- and underestimation is balanced inside the footprints. For the whole event the FBI supports a strong underestimation (see Table A1), strongly improved when adding the constraint (PC increases from 50% to 80%, FBI by the same amount). Interestingly, the Ka-band estimates, which should provide more accurate information in case of light precipitation, are not as accurate as the Ku-NS and the DPR-MS. The POD with constraint scores around 70% for

Ku-NS and DPR-MS estimates, a reasonably good value, since the GPM estimates have a small bias of less than 0.5 mm, but KaPR estimates are at only 55%. Without the constraint only 0.45 is reached, Ka-band is even worse, because of the zero rain estimation where the grid states very light rain. Indeed, not considering the gridded gauge data, but stations-only precipitation, would improve this result.

The second event (no. 9 on 8th of May, 2014) has even lighter rainfall than the first with a maximum of less than 1.5 mm. The series of footprints is given in Fig. 7. Nearly all stations inside the footprints indicate, that no precipitation was measured. The gridded WegenerNet precipitation however, shows some rainfall, which portends that a lot of information will be missed by the satellite.

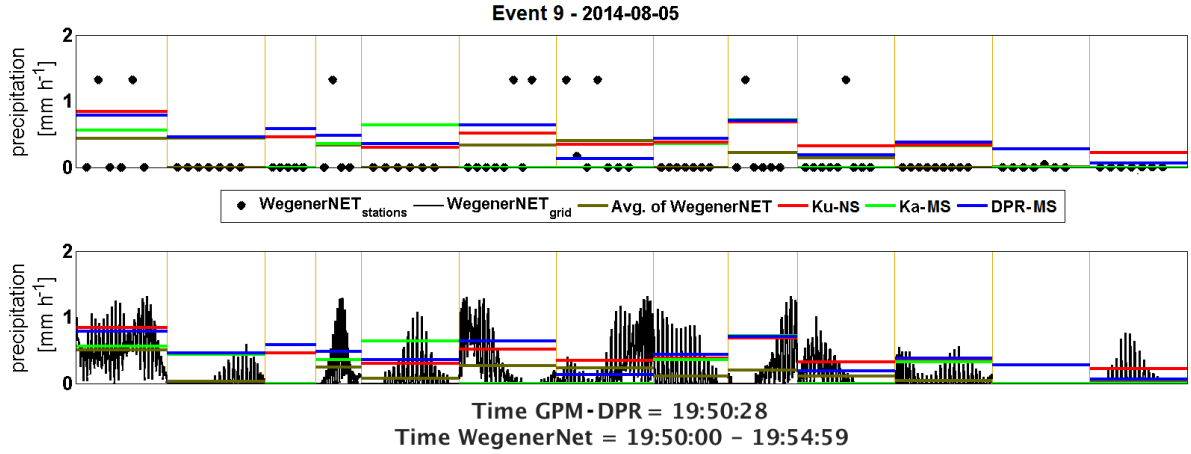

Figure 7. Series of footprints for Event 9 (8th of May, 2014) compared to station and grid data.

In contrast to Event no. 7, the GPM-DPR mirrors the gridded gauge data better than stations-only inside the footprint. The POD is at 1 for Ku-NS and DPR-MS, whereas the Ka-MS has a POD of only 0.64. The PC scores 0.85 for Ku-NS and DPR-MS and 0.69 for Ka-band estimates. The FBI suggests slight overestimation for the event, however the FAR is very low (between 0 and 0.15). When adding the constraint of the range, the Ka-band scores highest (0.55 compared to 0.27 for Ku-band and 0.36 for DPR-MS). The FBI and FAR now show an underestimation in Ku-band, Ka-band and DPR-MS estimates (FBI around 0.5, FAR between 0 (KaPR) and 40% (KuPR)), where Ka-band scores slightly better. This can be explained by the fact, that footprints out of range are treated as miss, which inverses the FBI's message. The Ka-band seems to be least sensitive to over-/underestimations. The correlation (Fig. 5) shows high discrepancies between the Ku-band, Ka-band and DPR-MS, with the Ka-MS being least accurate. A closer look at the event in the WegenerNet (Fig. A6, lag +0 min), points out that the event is hard to detect, since the precipitation occurs quite spotty over the whole area. Therefore, the satellite misses a lot of information that can only be provided by the gridded gauge data.

For Event no. 12, represented in Fig. 8, all three GPM-DPR products show relatively poor performance. Every footprint is heavily underestimated, and the radar estimates are within the range only in three out of twelve footprints.

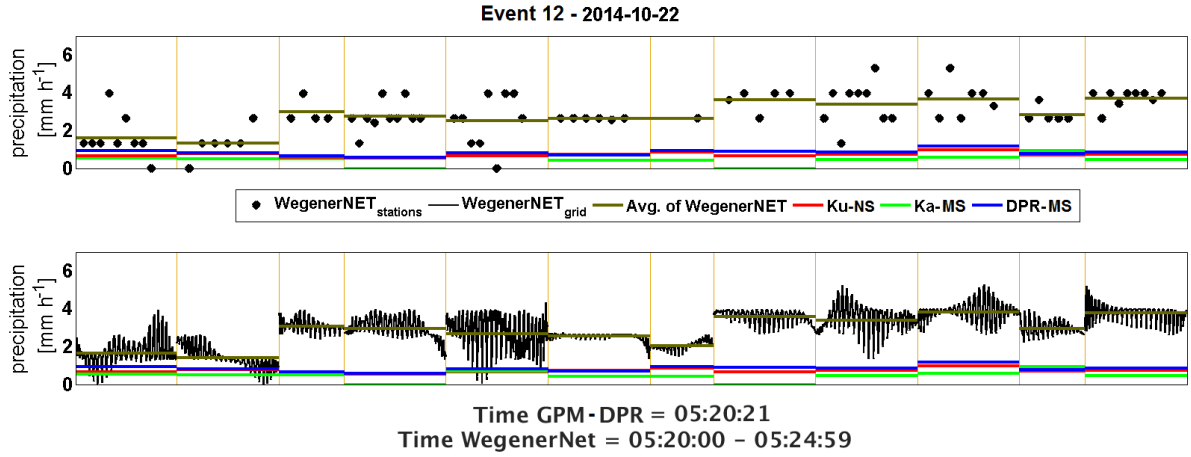

Figure 8. Series of footprints for Event 12 (22nd of October, 2014) compared to station and grid data.

The event contains uniformly distributed moderate rainfall (see figure A7 in the appendix), with hardly any station observing no-rain. The PC, FBI and POD are very high (between 83% and 100% without constraint), thus the fact, that it was rainy, is detected. However, the constrained POD discards all precipitation estimates. Ka-band information performs worst in terms of bias and correlation.

The opposite happens in Event no. 16, (2nd of May, 2016, Fig. 9), featuring moderate to heavy precipitation, up to 7 $\mathrm{mm\,h^{-1}}$.

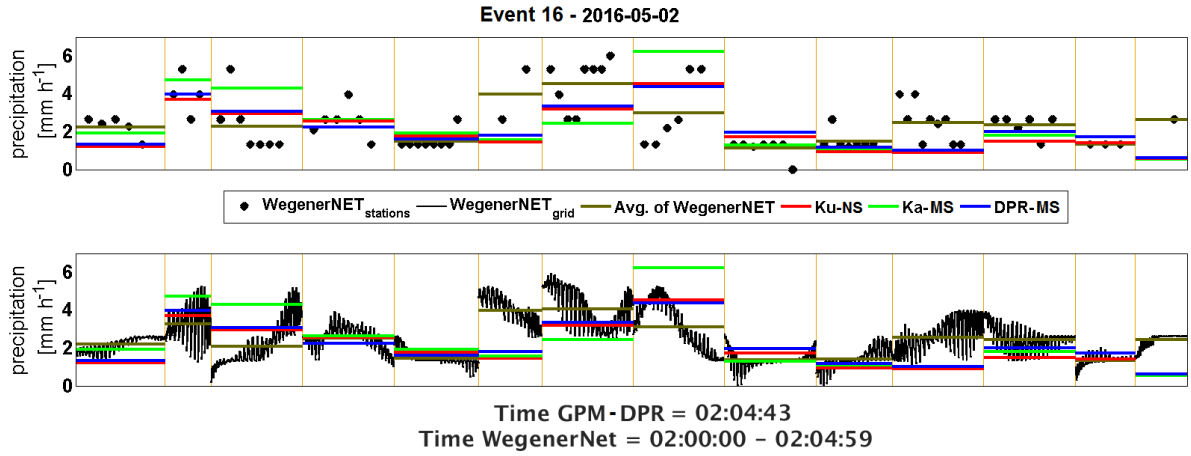

Figure 9. Series of footprints for Event 16 (2nd of May, 2016) compared to station and grid data.

The events shows a lot of variability (see Fig. 11 for 65 min of the rainfall) and is at a first glance almost perfectly mirrored by the radar estimates. The PC, FBI and POD is 100% for all products, the FAR is zero. The bias itself is quite low (highest for Ka-MS) and the correlation is close to 0.5. However, since there are no large scale variations within many footprints, the constrained POD drops to less than 0.6 for Ku-NS and DPR-MS. For Ka-MS, which is even out of the range of five footprints, it is less than 0.3. The FBI states an underestimation.

Remote sensing data may show a time lag error between rain drops from clouds and the surface rainfall. In order to investigate this effect, whether the GPM-DPR estimation was matched to the correct point in time for the rainfall event, a lag of ±30 min is applied and the correlation and the bias are determined. This is displayed in Fig. 10.

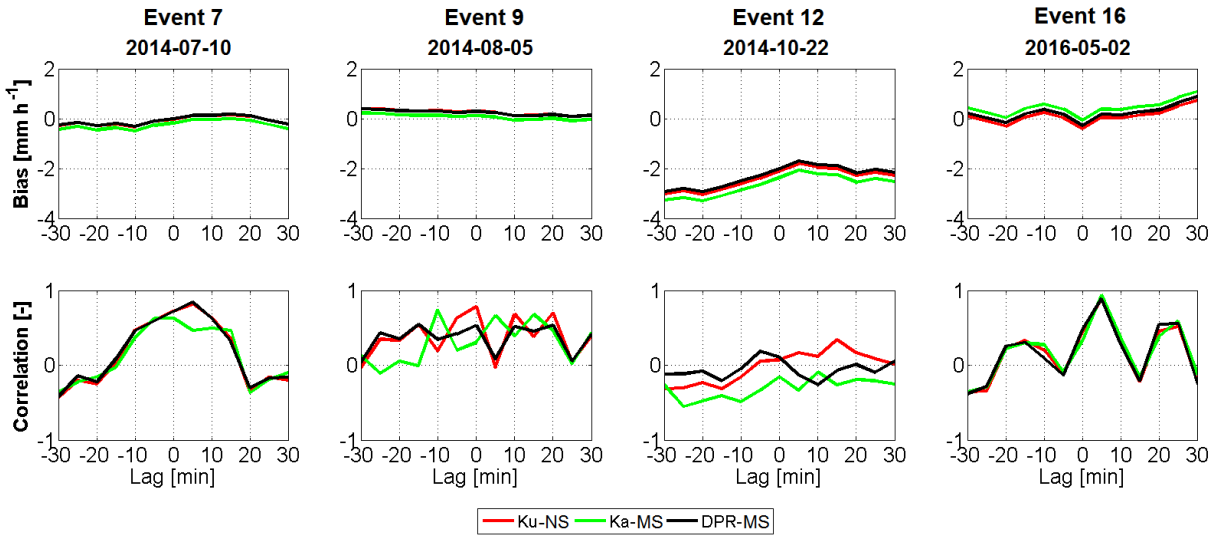

Figure 10. Bias and correlation for a lag of ±30 minutes for the example rainfall events.

For a perfectly matching event, the bias should be as close as possible to zero and the correlation should tend towards one, both occur for example for the Ku-band at a lag of +5 min in Event no. 16. But one cannot conclude, that the lag with the smallest bias shows also the highest correlation.

Event 7 and 9 have a very small bias due to their light and non-extensive rainfall. When shifting the WegenerNet ±30 min the bias stays at the same level, with its closest point to zero at a lag of +0 min. From that point of view, a perfect matching in time is achieved. In case of Event 9 the correlation shows a lot of variation between the three products, still the Ku-band has its peak at +0 min. Since there is a lot of information missed by the satellite, this event is hard to detect. In case of Event 7, the GPM-DPR footprints got exactly the characteristics of the WegenerNet at a lag of +5 min. A look at the lag +0 min and +5 min (Fig. A5) shows the similarities between the two lags. The fast decreasing correlation around the peak implies a fast moving precipitation event.

Event no. 12 is almost not correlated for the whole lag and also the bias is very high with only underestimated precipitation

rates.

For Event 16 a clear peak in the correlation is at a lag of +5 min, whereas -5 min and +15 min is almost not correlated. Thus, it was a quite fast moving rainfall, which underlines the importance of a correct tagging of rain rate estimates in time. The peak at +5 min lag can be explained in two ways. First the GPM-DPR measurements, which refer to a point in time, are taken at the very end of the WegenerNet interval. And second, the main characteristics of the whole WegenerNet which the satellite maps, did not shift from +0 min to +5 min, although the grid changed obviously (Fig. 11). One may compare with Fig. 2 to see which information is missed by the satellite.

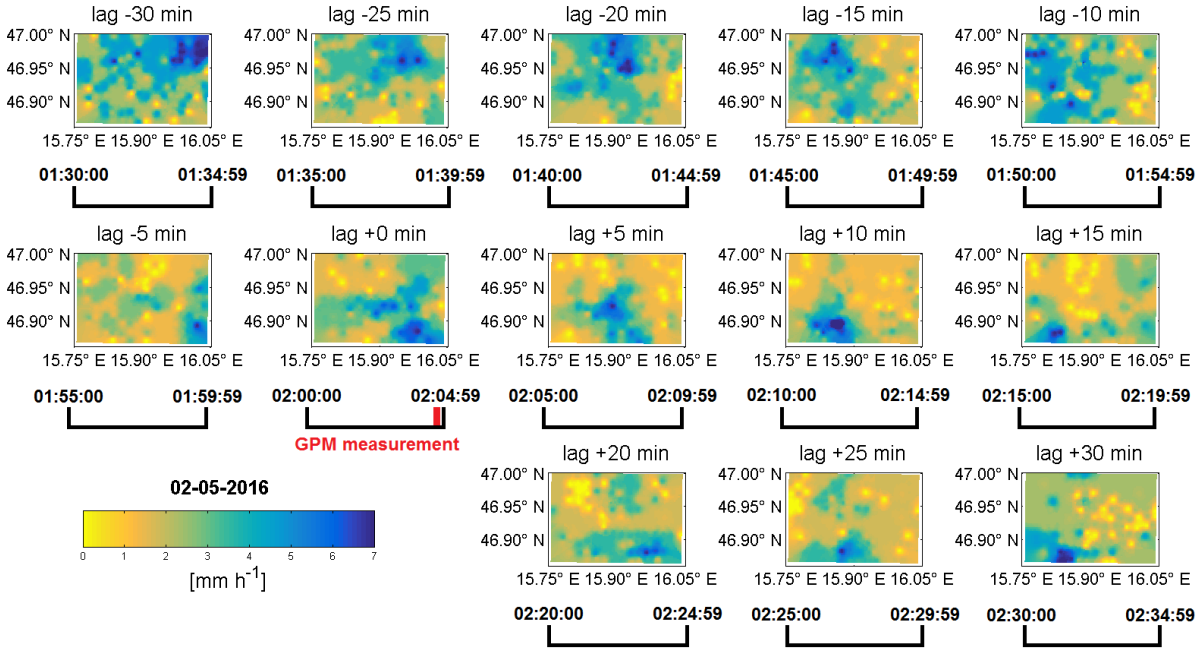

Figure 11. Evolution of Event 16 (2nd of May, 2016) with a lag of ±30 minutes.

5 Conclusions

In this study the radar estimates on both frequencies of the GPM-CO were evaluated using gauge measurement data from the WegenerNet network in southeastern Austria for the period of March–November of 2014 until 2017. The dense network provides the opportunity of evaluating the radar estimates not only amount-based but also on a level whether the satellite can observe small scale variability of rainfall events. Our results show that the evaluation using gridded gauge data provides more information than stations only. This plus of information helps to evaluate the GPM-DPR estimates and supports the quality of the satellites measurements in most cases. However, exceptions to that assumption can be found as well, especially in the case of light and spotty rainfall. One cannot infer the quality of the estimates from the amount of rainfall. In this study Ka-band

estimates perform best, probably due to the higher number of light rain events and their tendency of correctly mirroring zero rainfall. Consequently, Ka-band estimates tend to underestimation. Ku-band estimates and the dual frequency product perform vice versa. Considering the inter-footprint variability, all three products tend towards an under-representation of the precipitation. The correlation peak between the GPM-DPR and the WegenerNet is shifted in some events, however, this could be explained by the distribution of the rainfall event and which parts of the network's area the DPR cannot see. The probability of detection is over 70% for Ku-band-NS and DPR-MS, but only 50% for Ka-band-MS. When the constraint of an interval of $\pm$standard deviation is added, the POD for Ku-NS and DPR-MS estimates drops to less the 60%, the Ka-band keeps its level, showing that the Ku-NS and DPR-MS estimates tend to capture the precipitation, but largely biased.

The intra-event variations are captured from the satellite without clear characteristics, some events are resembled with a correlation close to one and some are almost not correlated. But, there is no event completely anti-correlated. Any systematic shifts (by moving the WegenerNet ± 30 min) could be explained by the gaps between the footprints.

Further studies on the GPM-DPR data and the WegenerNet, especially ones dealing with the detection of variations in small areas, would have to deal with the HS swath of the KaPR and DPR, because the amount of uncovered area inside the WegenerNet is drastically reduced.

Data availability. WegenerNet data are available at the WegenerNet data portal http://www.wegenernet.org/ in NetCDF format.
GPM-CO radar data sets are available at the PMM server http://pmm.nasa.gov/data-access/ delivered in HDF5 format.
Ku-band: doi:10.5067/GPM/DPR/KU/2A/05
Ka-band: doi:10.5067/GPM/DPR/KA/2A/05
DPR: doi:10.5067/GPM/DPR/GPM/2A/05

Appendix: Appendix A

Table A1 lists the statistical items from the derived from the contingency table for each event. In Fig. A1 and Fig. A2 a graphical representation of the WegenerNet gauge observations is given, that compares the station-wise mean to the grid mean inside the GPM-DPR footprints. They contain the same information. Figure A3 depicts the series of footprints containing the range of the grid in each footprint (inter footprint variability, marked by the blue line), the standard deviation of the WegenerNet in each footprint and the difference to the respective GPM-DPR estimation. Ideally, the difference should be less than the standard deviation, which itself is less than the range. Figure A4, A5 and A6 show the evolution of the rainfall events, that were analysed in detail.

Competing interests. The authors declare that they have no conflict of interest.

Acknowledgements. The study was funded by Austrian Science Fund (FWF) under research grant W 1256-G15 (Doctoral Programme Climate Change Uncertainties, Thresholds and Coping Strategies).

Table A1. Statistics derived from the contingency table for each event.

	PC			FBI			POD			FAR			POFD		
	Ku-NS	Ka-MS	DPR-MS	Ku-NS	Ka-MS	DPR-MS	Ku-NS	Ka-MS	DPR-MS	Ku-NS	Ka-MS	DPR-MS	Ku-NS	Ka-MS	DPR-MS
Event 1	0.50	0.58	0.50	1.29	0.29	1.29	0.71	0.29	0.71	0.44	0	0.44	0.80	0	0.80
Event 2	0.58	0.58	0.58	1.20	0	0.80	0.60	0	0.40	0.50	-	0.50	0.43	0	0.29
Event 3	0.50	0.33	0.50	0.45	0.27	0.45	0.45	0.27	0.45	0	0	0	0	0	0
Event 4	1	1	1	-	-	-	-	-	-	-	-	-	0	0	0
Event 5	0.17	0.50	0.33	0.25	0.25	0	0	0.25	0	1	0	-	0.50	0	0
Event 6	0	1	0	Inf	-	Inf	-	-	-	1	-	1	1	0	1
Event 7	0.50	0.43	0.50	0.55	0.27	0.55	0.45	0.27	0.45	0.17	0	0.17	0.33	0	0.33
Event 8	0.93	1	0.93	Inf	-	Inf	-	-	-	1	-	1	0.07	0	0.07
Event 9	0.85	0.69	0.85	1.18	0.64	1.18	1	0.64	1	0.15	0	0.15	1	0	1
Event 10	0.69	0.92	0.69	Inf	Inf	Inf	-	-	-	1	1	1	0.31	0.08	0.30
Event 11	0.92	1	0.92	2	1	2	1	1	1	0.50	0	0.50	0.08	0	0.08
Event 12	1	0.83	1	1	0.83	1	1	0.83	1	0	0	0	-	-	-
Event 13	0.86	0.86	0.86	Inf	Inf	Inf	-	-	-	1	1	1	0.14	0.14	0.14
Event 14	0.40	1	0.60	1.50	1	2	0.50	1	1	0.67	0	0.50	0.67	0	0.67
Event 15	1	0.15	1	1	0.15	1	1	0.15	1	0	0	0	-	-	-
Event 16	1	1	1	1	1	1	1	1	1	0	0	0	-	-	-
Event 17	0.62	0.69	0.62	0.89	0.56	0.89	0.67	0.56	0.67	0.25	0	0.25	0.50	0	0.50
Event 18	0.62	0.62	0.62	0.86	0.57	0.86	0.57	0.43	0.57	0.33	0.25	0.33	0.33	0.17	0.33
Event 19	0.54	0.69	0.54	1.86	1	1.86	1	0.71	1	0.46	0.29	0.46	1	0.33	1
Event 20	0.64	0.29	0.57	0.75	0.17	0.83	0.67	0.17	0.67	0.11	0	0.20	0.50	0	1
Event 21	1	1	0	-	-	Inf	-	-	-	-	-	1	0	0	1
Event 22	1	1	1	-	-	-	-	-	-	-	-	-	0	0	0

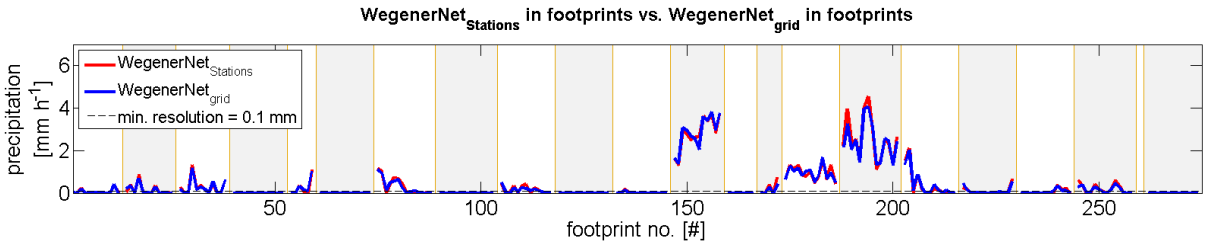

Figure A1. WegenerNet station data compared to the grid data in the footprints (average respectively).

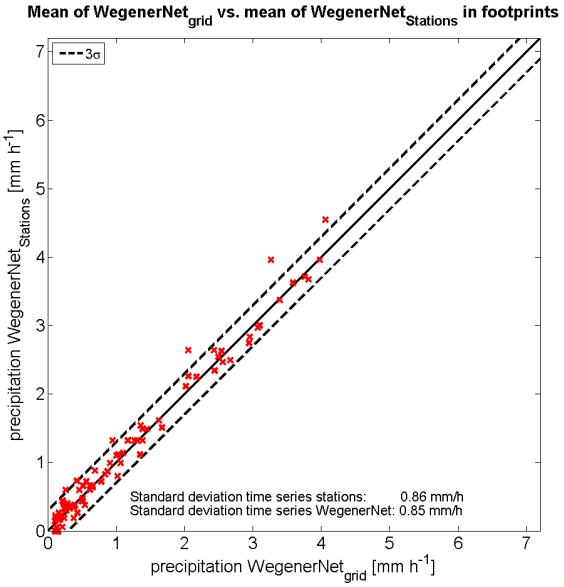

Figure A2. WegenerNet station observations as a function of the WegenerNet grid data. The dashed line denotes three times the standard deviation of the measurements.

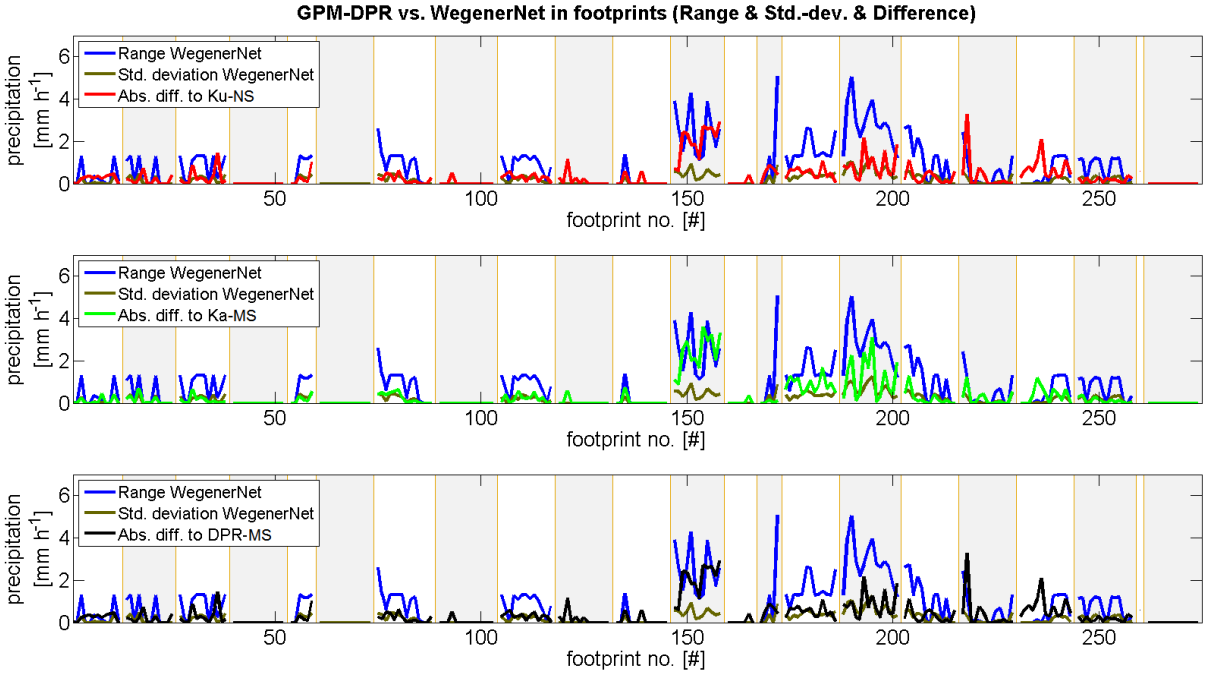

Figure A3. Range and standard deviation of the WegenerNet in the respective footprints and absolute difference between the GPM-DPR measurements and the average of the WegenerNet in the footprints.

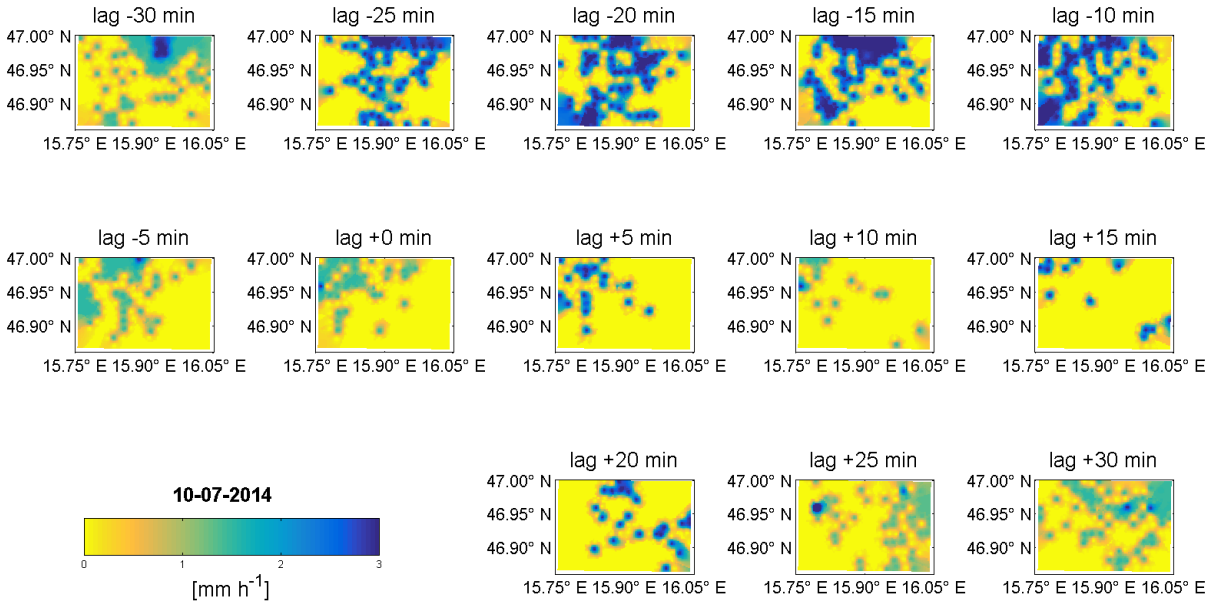

Figure A4. Evolution of Event 7 (10^{th} of July, 2014) with a lag of $\pm$30 minutes.

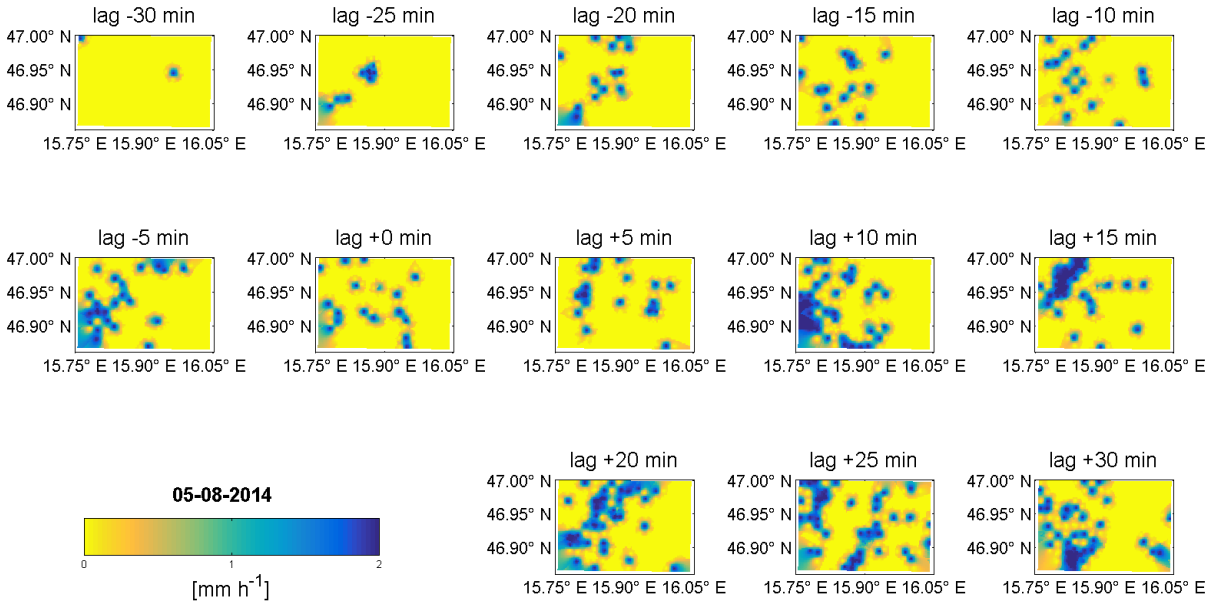

Figure A5. Evolution of Event 9 (8th of May, 2014) with a lag of ±30 minutes.

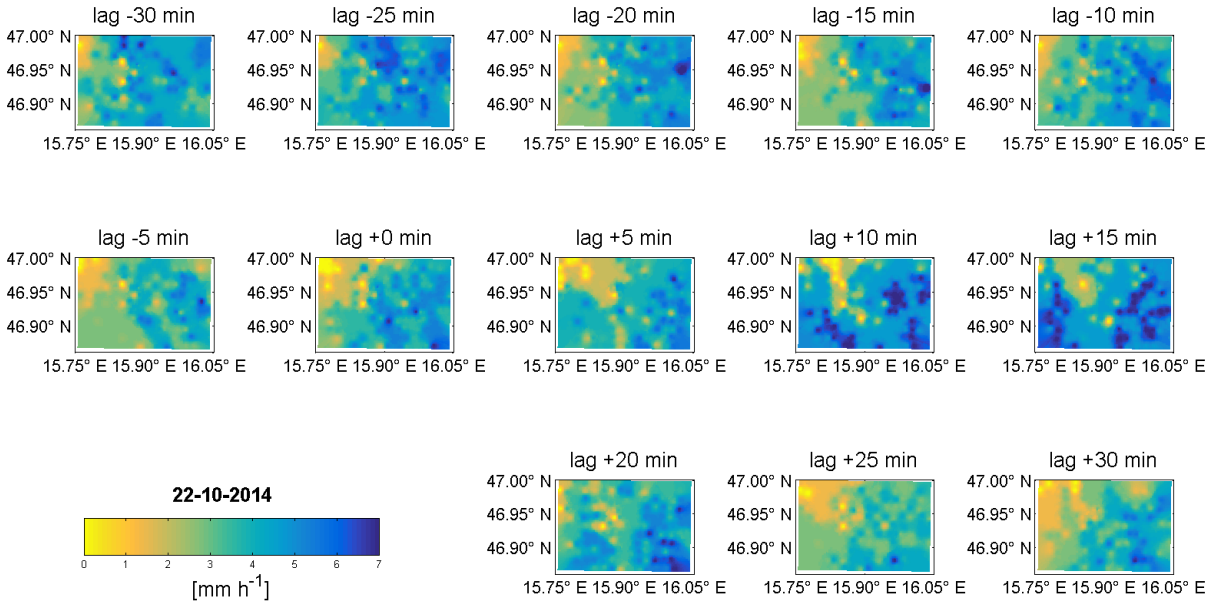

Figure A6. Evolution of Event 12 (22nd of October, 2014) with a lag of $\pm$30 minutes.

References

Amitai, E., Unkrich, C. L., Goodrich, D. C., Habib, E., Thill, B.: Assessing Satellite-Based Rainfall Estimates in Semiarid Watersheds Using the USDA-ARS Walnut Gulch Gauge Network and TRMM PR, 2012, J. Hydrometeor., 13, 1579–1588, doi:10.1175/JHM-D-12-016.1

Casella, D., Panegrossi, G., Sanò, P., Marra, A. C., Dietrich, S., Johnson, B. T., Kulie, M. S.: Evaluation of the GPM-DPR snowfall detection capability: Comparison with CloudSat-CPR, 2017, Atmospheric Research, 197, 64-75, doi:10.1016/j.atmosres.2017.06.018

Hamada, A. and Takayabu, Y. N.: Improvements in Detection of Light Precipitation with the Global Precipitation Measurement Dual-Frequency Precipitation Radar (GPM DPR), 2016, J. Atmospheric Ocean. Technol., 33 (4), 653–667, doi:10.1175/JTECH-D-15-0097.1

Hou, A. Y., Kakar, R. K., Neeck, A. A., Azarbarzin, A., Kummerow, C. D., Kojima, M., Oki, R., Nakamura, K., Iguchi, T.: The Global Precipitation Measurement Mission, 2014, Bull.Amer.Meteor. Soc., 95, 701-722, doi:10.1175/BAMS-D-13-00164.1

Iguchi, T., Seto, S., Meneghini, R., Yoshida, N., Awaka, J., Le, M., Chandrasekar, V., Kubota, T.: GPM/DPR Level-2 Algorithm Theoretical Basis Document, 2010, revised 2015

Japan Aerospace Exploration Agency (JAXA): GPM Data Utilization Handbook, GPM Data Utilization Handbook, 2017

Kidd, C., Tan, J., Kirstetter, P.-E., Petersen, W. A.: Validation of the Version 05 Level 2 precipitation products from the GPM Core Observatory and constellation satellite sensors, 2017, Q. J. R. Meteorol. Soc., doi:10.1002/qj.3175

Kirchengast, G., Kabas, T., Leuprecht, A., Bichler, C., and Truhetz, H.: WegenerNet: A pioneering high-resolution network for monitoring weather and climate, 2014, Bull. Amer. Meteor. Soc., 95, 227–242, doi:10.1175/BAMS-D-11-00161.1

O, S., Foelsche, U., Kirchengast, G., Fuchsberger, J., Tan, J., Petersen, W. A.: Evaluation of GPM IMERG Early, Late, and Final rainfall estimates using WegenerNet gauge data in southeastern Austria, 2017, Hydrol. Earth Syst. Sci., 21 (12), 6559–6572, doi:10.5194/hess-21-6559-2017

O, S., Foelsche, U., Kirchengast, G., Fuchsberger, J.: Validation and correction of rainfall data from the WegenerNet high density network in southeast Austria, 2018, J. Hydrol., 556, 1110-1122, doi:10.1016/j.jhydrol.2016.11.049

O., S. and Foelsche U.: Assessment of spatial uncertainty of heavy local rainfall using a dense gauge network, 2018, Hydrol. Earth Syst. Sci. Discuss., doi:10.5194/hess-2018-517

Seto, I. and Iguchi, T.: Intercomparison of Attenuation Correction Methods for the GPM Dual-Frequency Precipitation Radar, 2014, J. Atmos. Oceanic Technol., 32, 915–926, doi:10.1175/JTECH-D-14-00065.1

Jackson, G.: NASA's Global Precipitation Measurement (GPM) Mission: Observing Rain and Snow for Science and Society, Talk at EUMETRAIN 2015

Jackson, G., Petersen, W. A., Berg, W., Kidd, C., Stocker, E. F., Kirschbaum, D. B., Kakar, R., Braun, S. A., Huffman, G. J., Iguchi, T., Kirstetter, P.-E., Kummerow, C., Meneghini, Oki, R., Olson, W. S., Takayabu, Y. N., Furukawa, K., Wilheit, T.: The Global Precipitation Measurement (GPM) Mission for Science and Society, 2016, Bulletin of the American Meteorological Society. 98. doi:10.1175/BAMS-D-15-00306.1

Speirs, P., Gabella, M. and Berne, A.: A comparison between the GPM dual-frequency precipitation radar and ground-based radar precipitation rate estimates in the Swiss Alps and Plateau, 2017, J. Hydrometeorol., 18, 1247–1269, doi:/10.1175/JHM-D-16-0085.1

Szeberényi, K.: Analysis of WegenerNet precipitation data and quality evaluation for case studies and climatologies, 2014, Sci. Rep. 58-2014, Wegener Center for Climate and Global Change, Graz, Austria, http://wegcwww.uni-graz.at/publ/wegcreports/2014/WCV-SciRep-No58-KSzeberenyi-Mar2014.pdf, last access: Oct. 2018

Tan, J., Petersen, W. A., Kirchengast, G., Goodrich, D. C., Wolff, D. B.: Evaluation of Global Precipitation Measurement Rainfall Estimates against Three Dense Gauge Networks, 2017, doi.org/10.1175/JHM-D-17-0174.1

Toyoshima, K., Masunaga, H. and Furuzawa, F. A.: Early evaluation of Ku- and Ka-Band Sensitives for the Global Precipitation Measurement (GPM) Dual-Frequency Radar (DPR), 2015, SOLA, 11, 14-17, doi:10.2151/sola.2015-004

Appending the paper, precipitation maps of all events contrasting the WegenerNet and the GPM-DPR estimates, are given here.

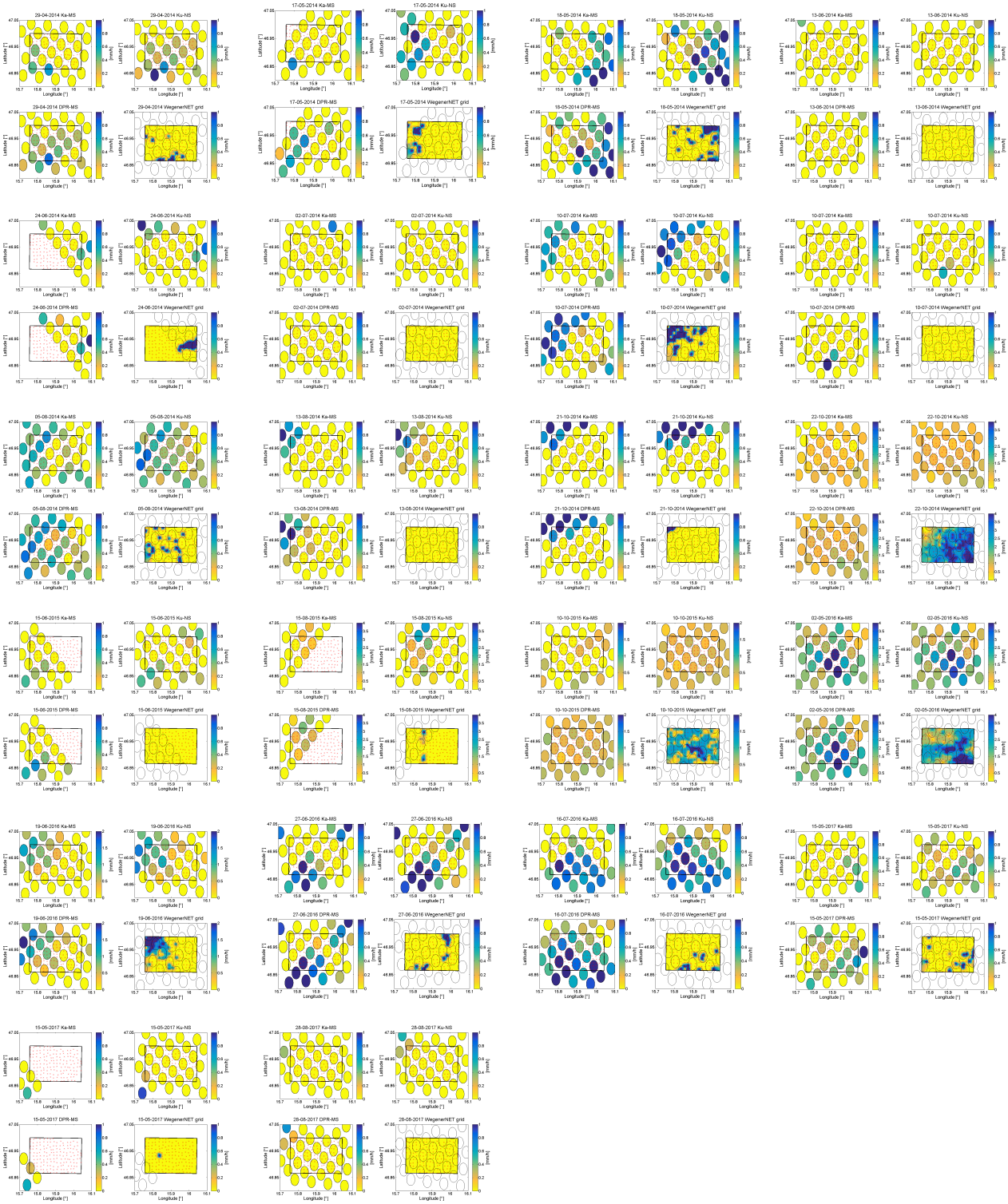

References

ESA (2017): Earth Observation Portal (eoPortal) - GPM satellite mission:
`https://directory.eoportal.org/web/eoportal/satellite-missions/g/gpm`

Hou, A. Y., Kakar, R. K., Neeck, A. A., Azarbarzin, A., Kummerow, C. D., Kojima, M., Oki, R., Nakamura, K., Iguchi, T.: The Global Precipitation Measurement Mission, 2014, Bull.Amer.Meteor. Soc., 95, 701-722, doi:10.1175/BAMS-D-13-00164.1

Iguchi Toshi: Radar Measurement of Precipitation from Space: TRMM/PR and GPM/DPR rain retrieval algorithms, Riken, Kobe, 2017

Iguchi Toshio: Spaceborne precipitation RADARs in TRMM and GPM, 31st International Conference on Radar Meteorology, 2003

Jameson, A. R. and Kostinski, A. B.: What is a Raindrop Size Distribution?, Bulletin of the American Meteorological Society, Vol. 82, No. 6, 2001

Japan Aerospace Exploration Agency (JAXA): GPM Data Utilization Handbook, GPM Data Utilization Handbook, 2017

Japan Aerospace Exploration Agency (JAXA), National Aeronautics and Space Administration (NASA): GPM Press Kit, 2014

Kabas Thomas: WegenerNet Klimastationsnetz Region Feldbach: Experimenteller Aufbau und hochauflösende Daten für die Klima- und Umweltforschung, 2012, Dissertation Universität Graz

Kirchengast, G., Kabas, T., Leuprecht, A., Bichler, C., and Truhetz, H.: WegenerNet: A pioneering high-resolution network for monitoring weather and climate, 2014, Bull. Amer. Meteor. Soc., 95, 227-242, https://doi.org/10.1175/BAMS-D-11-00161.1

O, S., Foelsche, U., Kirchengast, G., Fuchsberger, J., Tan, J., Petersen, W. A.: Evaluation of GPM IMERG Early, Late, and Final rainfall estimates using WegenerNet gauge data in southeastern Austria, 2017,
Hydrol. Earth Syst. Sci., 21 (12), 6559–6572, doi:10.5194/hess- 21-6559-2017

O, S., Foelsche, U., Kirchengast, G., Fuchsberger, J.: Validation and correction of rainfall data from the WegenerNet high density network in southeast Austria, 2018,
J. Hydrol., 556, 1110-1122,doi:10.1016/j.jhydrol.2016.11.049

Jackson, G.: NASA's Global Precipitation Measurement (GPM) Mission: Observing Rain and Snow for Science and Society, Talk at EUMETRAIN 2015

Jackson, G., Petersen, W. A., Berg, W., Kidd, C., Stocker, E. F., Kirschbaum, D. B., Kakar, R., Braun, S. A., Huffman, G. J., Iguchi, T., Kirstetter, P.-E., Kummerow, C., Meneghini, Oki, R., Olson, W. S., Takayabu, Y. N., Furukawa, K., Wilheit, T.: The Global Precipitation Measurement (GPM) Mission for Science and Society, 2016, Bulletin of the American Meteorological Society. 98. 10.1175/BAMS-D-15-00306.1

Szeberényi, K.: Analysis of WegenerNet Precipitation Data and Quality Evaluation for Case Studies and Climatologies, 2014

Index of abbreviations

Abbreviation	Description
ADCS	Attitude Determination and Control Subsystem
AMT	Atmospheric Measurement Techniques
C&DHS	Command & Data Handling Subsystem
CNES	Centre National d'Études Spatiales
DPR	Dual frequency Precipitation Radar
DSD	Drop Size Distribution
EUMETSAT	European Organisation for the Exploitation of Meteorological Satellites
EOS	Earth Observation System
EPS	Electrical Power Subsystem
GMI	GPM Micorwave Imager
GSFC	Goddard Space Flight Center
GPM	Global Precipitation Measurement
GPM-CO	Global Precipitation Measurement - Core Observatory
GPS	Global Positioning System
ESA	European Space Agency
ISRO	Indian Space Research Organisation
JAXA	Japan Aerospace Exploration Agency
KaPR	Ka-band Precipitation Radar
KuPR	Ku-band Precipitation Radar
MOC	Mission Operation Center
NASA	National Aeronautics and Space Administration
NOAA	National Oceanic and Atmospheric Administration
RCS	Reaction Control Subsystem
RF	Radio Frequency
TCS	Thermal Control Subsystem
TDRS	Tracking and Data Relay Satellite
TRMM	Tropical Rainfall Measurement Misson